Technical University of Denmark

DTU

Highly Active and Specific Tyrosine Ammonia-Lyases from Diverse Origins Enable Enhanced Production of Aromatic Compounds in Bacteria and Saccharomyces cerevisiae

Jendresen, Christian Bille; Stahlhut, Steen Gustav; Li, Mingji; Gaspar, Paula; Siedler, Solvej; Förster, Jochen; Maury, Jerome; Borodina, Irina; Nielsen, Alex Toftgaard

DTU Library
Technical Information Center of Denmark

Highly Active and Specific Tyrosine Ammonia-Lyases from Diverse Origins Enable Enhanced Production of Aromatic Compounds in Bacteria and *Saccharomyces cerevisiae*

Christian Bille Jendresen, Steen Gustav Stahlhut, Mingji Li, Paula Gaspar, Solvej Siedler, Jochen Förster, Jérôme Maury, Irina Borodina, Alex Toftgaard Nielsen

The Novo Nordisk Foundation Center for Biosustainability, Technical University of Denmark, Hørsholm, Denmark

Phenylalanine and tyrosine ammonia-lyases form cinnamic acid and *p*-coumaric acid, which are precursors of a wide range of aromatic compounds of biotechnological interest. Lack of highly active and specific tyrosine ammonia-lyases has previously been a limitation in metabolic engineering approaches. We therefore identified 22 sequences *in silico* using synteny information and aiming for sequence divergence. We performed a comparative *in vivo* study, expressing the genes intracellularly in bacteria and yeast. When produced heterologously, some enzymes resulted in significantly higher production of *p*-coumaric acid in several different industrially important production organisms. Three novel enzymes were found to have activity exclusively for phenylalanine, including an enzyme from the low-GC Gram-positive bacterium *Brevibacillus laterosporus*, a bacterial-type enzyme from the amoeba *Dictyostelium discoideum*, and a phenylalanine ammonia-lyase from the moss *Physcomitrella patens* (producing 230 μM cinnamic acid per unit of optical density at 600 nm [OD_{600}]) in the medium using *Escherichia coli* as the heterologous host). Novel tyrosine ammonia-lyases having higher reported substrate specificity than previously characterized enzymes were also identified. Enzymes from *Herpetosiphon aurantiacus* and *Flavobacterium johnsoniae* resulted in high production of *p*-coumaric acid in *Escherichia coli* (producing 440 μM *p*-coumaric acid OD_{600} unit^{-1} in the medium) and in *Lactococcus lactis*. The enzymes were also efficient in *Saccharomyces cerevisiae*, where *p*-coumaric acid accumulation was improved 5-fold over that in strains expressing previously characterized tyrosine ammonia-lyases.

S mall organic molecules of biotechnological interest include aromatic structures that are derived from *p*-coumaric acid (pHCA). pHCA can be formed from phenylalanine either through deamination to cinnamic acid (CA) by phenylalanine ammonia-lyase (PAL; EC 4.3.1.24) and subsequent hydroxylase activity by *trans*-cinnamate-4-monooxygenase or through deamination of tyrosine by tyrosine ammonia-lyase (TAL; EC 4.3.1.23) (Fig. 1). Considering that the route from phenylalanine requires activity of a P450 enzyme, which has been shown to be the limiting step in previous engineering strategies (1, 2), deamination of tyrosine for production of pHCA may be preferred in microbial cell factories. Tyrosine ammonia-lyases (TAL) have been employed for the production of plant biochemicals and aromatic compounds, e.g., for pHCA itself (3–5), or in the production of stilbenes, such as resveratrol (6, 7), flavonoids, such as naringenin (8, 9), cinnamoyl anthranilates (10), or plastic precursors, such as *p*-hydroxystyrene (11, 12), yet the TAL reaction may be the limiting step (10, 13).

Due to the significant interest in production of phenolic compounds in biotechnological processes, we aimed at increasing the range of characterized phenylalanine ammonia-lyases (PAL) and tyrosine ammonia-lyases (TAL), and in particular at identifying the optimal TAL for use in microbial cell factories. Several enzymes have previously been characterized both *in vivo* and *in vitro*, and the data are available from both patent and scientific literature (3, 14–32). However, the conditions of kinetic analysis are often quite different and may not represent the extent to which the enzymes perform *in vivo*. Therefore, we decided to evaluate a range of previously identified enzymes, and expanded our analysis to novel enzymes selected from available sequence data. Identification of TAL enzymes based solely on sequence information is not straightforward, since the sequences do not provide unambig-

uous prediction of substrate specificity. This is illustrated by the fact that hypothetical genes whose predicted products have homology to aromatic amino acid ammonia-lyases are often simply annotated as being histidine ammonia-lyases without experimental evidence of their substrate specificity.

Phenylalanine and tyrosine ammonia-lyases are members of a family that either have a lyase activity that forms α,β-unsaturated acids from amino acids by elimination of ammonia or a mutase activity that forms β-amino acids. The aromatic amino acid ammonia-lyases (here XAL) in this family are classified by their substrate specificity as being histidine ammonia-lyases (HAL; histidase; EC 4.3.1.3), tyrosine ammonia-lyases (TAL; EC 4.3.1.23), phenylalanine ammonia-lyases (PAL; EC 4.3.1.24), or phenylalanine/tyrosine ammonia-lyases (PAL/TAL; EC 4.3.1.25) (Fig. 1).

FIG 1 Aromatic amino acid ammonia-lyases and aminomutases. Phenylalanine (Phe) may be converted into β-phenylalanine (β-Phe) by phenylalanine aminomutase (PAM) or deaminated to cinnamic acid (CA). Similarly, tyrosine (Tyr) may be converted to β-tyrosine by tyrosine aminomutase (TAM) or *p*-coumaric acid (pHCA) by tyrosine ammonia-lyase (TAL). pHCA may also be formed from CA by cinnamate 4-hydroxylase (C4H). Histidine (His) may be deaminated to urocanic acid by histidine ammonia-lyase (HAL).

Enzymes categorized as acting on either of the structurally similar amino acids tyrosine or phenylalanine often have some activity for the other substrate as well (16, 32) or for similar compounds, such as 3,4-dihydroxy-L-phenylalanine (L-dopa) (22). Homologous and structurally similar enzymes are tyrosine 2,3-aminomutases (TAM; EC 5.4.3.6) and phenylalanine aminomutase (PAM; EC 5.4.3.11) (33–35). The enzyme activities are difficult to predict based on primary sequence, as all enzymes contain a prosthetic group, 3,5-dihydro-5-methylidene-4H-imidazol-4-one (MIO), formed by the cyclization of the sequential amino acids alanine, serine, and glycine (22, 36–38).

Here we compared previously described and commonly used enzymes—RsTAL from *Rhodobacter sphaeroides* (1, 39), RcTAL from *Rhodobacter capsulatus* (9, 18), BagA from *Streptomyces* sp. (40), SeSam8 from *Saccharothrix espanaensis* (21), RmXAL from *Rhodotorula mucilaginosa* (41–43), and other fungal enzymes—for enzymatic activity *in vivo* together with 11 uncharacterized enzymes.

MATERIALS AND METHODS

Bioinformatic methods. The nonredundant protein database in GenBank was searched using BLASTP 2.2.28+ using four known enzymes having

TAL activity: RsTAL from *Rhodobacter sphaeroides*, RmXAL from *Rhodotorula mucilaginosa*, S_bagA from *Streptomyces* sp., and SeSam8 from *Saccharothrix espanaensis*. To limit the list of BLAST hits to the most likely correctly annotated sequences, duplicates were removed and the resulting hits were limited to those having homology over the central part of the sequence covering the catalytically important residues, ranging from the alanine-serine-glycine triplet forming the MIO prosthetic group (A149 in RsTAL) (see Fig. S1 in the supplemental material) to the tyrosine stabilizing the MIO group (Y303 in RsTAL) and to a minimum length of 300 amino acids. We grouped the hits into clusters using H-CD-HIT in the CD-HIT suite (44), with three hierarchical rounds of clustering: 90%, 60%, and 40% amino acid identity, yielding 107 clusters. Assignment to phyla was done by reconstructing taxonomy trees from the NCBI taxonomy database. Synteny was analyzed using GCView (45) with input sequences being PSI-BLAST results for RsTAL (GI 126464011) from *Rhodobacter sphaeroides*, PYP (GI 409511), 4-coumarate-CoA ligase (4CL; GI 121590003) from *Halorhodospira halophila*, and the urocanate hydratase (*hutU*) protein of *Bacillus subtilis* (GI 603769) retrieved from the nonredundant database using standard parameters. Phylogenetic trees were constructed in MEGA6 (46) using the maximum-likelihood method based on a JTT matrix-based model (47) on Clustal Omega (48)-aligned sequences and an initial tree constructed by the neighbor-joining method.

Strains and media. (i) Media. *Escherichia coli* strains were routinely grown at 37°C on plates or in liquid culture in either lysogeny broth (LB) or 2×YT medium (16 g liter^{-1} Bacto tryptone, 10 g liter^{-1} Bacto yeast extract, 5 g liter^{-1} NaCl; adjusted to pH 7.0 with NaOH) with antibiotics when appropriate. Liquid cultures were incubated with aeration in an orbital shaker (250 rpm). For analysis of production rates, *E. coli* strains were grown in M9 minimal medium with 0.2% glucose. Growth was measured by following the optical density at 600 nm (OD$_{600}$).

Saccharomyces cerevisiae strains were routinely grown in synthetic dropout medium lacking histidine for selection of DNA integration or lacking uracil for selection of episomal plasmids. For production analysis, strains were grown either in the Feed-In-Time (FIT) synthetic fed-batch medium M-Sc.syn-1000 from m2p-labs GmbH (Germany) or in a defined minimal medium (49) based on Delft medium (50) supplemented with 76 mg liter^{-1} uracil and 380 mg liter^{-1} leucine or 25 mg liter^{-1} histidine and 75 mg liter^{-1} leucine at 30°C and 250 rpm.

For molecular biology procedures, *Lactococcus lactis* strains were cultivated as batch cultures (flasks) without aeration in M17 medium (Difco, USA) supplemented with 0.5% glucose (wt/vol) at 30°C. To assess pHCA production, strains were grown as static cultures in chemically defined medium (CDM) (51) containing 1% glucose (wt/vol) without pH control (initial pH 6.5 or 7.0) and supplemented with 1.7 or 3.7 mM L-tyrosine. Plasmid selection was achieved by addition of 5 μg ml^{-1} chloramphenicol to the growth medium. Growth was monitored by measuring OD$_{600}$.

(ii) DNA and molecular biology tools. DNA oligonucleotide primers (listed in Table 1) were purchased from Integrated DNA Technologies. Synthetic genes, codon optimized for expression in *E. coli*, *L. lactis* or *S. cerevisiae*, were ordered from GeneArt (Life Technologies). General molecular techniques were performed essentially as described elsewhere (52). Restriction enzymes, T4 DNA ligase, DNA polymerases, and Gibson Assembly master mix were obtained from New England BioLabs or Thermo Scientific and used according to the supplier's instructions. DNA purification was done using Macherey-Nagel kits, except for plasmid purification from *L. lactis*. Lactococcal plasmid DNA isolation was carried out using the QIAprep spin miniprep kit (Qiagen, United Kingdom) for small-scale purifications with the following modifications: the bacterial pellet was resuspended in Birnboim A solution (53), containing 5 mg ml^{-1} lysozyme and 30 μg ml^{-1} RNase I, and incubated at 55°C for 10 to 15 min before addition of buffer P2.

(iii) Cloning for expression in *Escherichia coli*. Genes optimized for *E. coli* (see Table S1 in the supplemental material) were amplified using the oligonucleotides shown in Table 1 and cloned into pCDFDuet-1 (Novagen) as follows. The plasmid was digested with NdeI and BglII and gel

TABLE 1 DNA oligonucleotides used in this study

Oligonucleotide	Gene	Direction	Sequence	Restriction site[a]	Use (reference)[b]
CBJP483	RsTAL	Forward	CATCTTAGTATATTAGTTAAGTATAAGAGGAGATATACATATGCTGGCAA TGAGCCCT		Ec
CBJP484	RsTAL	Reverse	TGGCCGGCCGATATCCAATTGATTAAACCGGACTCTGTTGC		Ec
CBJP485	S_BagA	Forward	CATCTTAGTATATTAGTTAAGTATAAGAAGGAGATATACATATGAAAATTG ATGGTCGTGGTCTG		Ec
CBJP486	S_BagA	Reverse	TGGCCGGCCGATATCCAATTGATTACAGATTACCGCCTGCAC		Ec
CBJP487	RmXAL	Forward	CATCTTAGTATATTAGTTAAGTATAAGAAGGAGATATACATATGGCACCG AGCGGTTGATAGC		Ec
CBJP488	RmXAL	Reverse	TGGCCGGCCGATCCATCCAATTGATTAGGCCATCATTTTAACCAGAACC		Ec
CBJP535	SeSam8	Forward	CATCTTAGTATATTAGTTAAGTATAAGAAGGAGATATACATATGACCCAG GTTGTTGAACG		Ec
CBJP536	SeSam8	Reverse	TGGCCGGCCGATATCCAATTGATTAGCCAAAATCTTTACCATCTGC		Ec
CBJP537	BlPAL	Forward	CATCTTAGTATATTAGTTAAGTATAAGAAGGAGATATACATATGAGCCA GGTTGCACTG		Ec
CBJP538	BlPAL	Reverse	TGGCCGGCCGATATCCAATTGATTAATCATTCACATTCTGATCATGAATTTC		Ec
CBJP539	R_XAL	Forward	CATCTTAGTATATTAGTTAAGTATAAGAAGGAGATATACATATGCGTAGCG AACAGCTGA		Ec
CBJP540	R_XAL	Reverse	TGGCCGGCCGATATCCAATTGATTAGGCCAGCAGTTCAATCA		Ec
CBJP541	PpPAL	Forward	CATCTTAGTATATTAGTTAAGTATAAGAAGGAGATATACATATGCACGA TGATAACACCAGC		Ec
CBJP542	PpPAL	Reverse	TGGCCGGCCGATATCCAATTGATTAACAGCTTGCGCGTGCGCTAAAC		Ec
CBJP543	LbTAL	Forward	CATCTTAGTATATTAGTTAAGTATAAGAAGGAGATATACATATGCCT CGTTTTTGTCCGA		Ec
CBJP544	LbTAL	Reverse	TGGCCGGCCGATATCCAATTGATTAATCGTTCGGGGTCATAACC		Ec
CBJP545	IITAL	Forward	CATCTTAGTATATTAGTTAAGTATAAGAAGGAGATATACATATGACCACCT CCATTATTGC		Ec
CBJP546	IITAL	Reverse	TGGCCGGCCGATATCCAATTGATTATGCGGTTCTTGATACAG		Ec
CBJP547	DdPAL	Forward	CATCTTAGTATATTAGTTAAGTATAAGAAGGAGATATACATATGATCGAAA CCAACCACA		Ec
CBJP548	DdPAL	Reverse	TGGCCGGCCGATATCCAATTGATTACAGGTTAATAAAGTCCA		Ec
CBJP549	SrXAL	Forward	CATCTTAGTATATTAGTTAAGTATAAGAAGGAGATATACATATGAGCAC CCGAGCGCA		Ec
CBJP550	SrXAL	Reverse	TGGCCGGCCGATATCCAATTGATTATGCGGTCGGAGGGTAAC		Ec
CBJP551	L_XAL	Forward	CATCTTAGTATATTAGTTAAGTATAAGAAGGAGATATACATATGACCC TGACCCCGAC		Ec
CBJP552	L_XAL	Reverse	TGGCCGGCCGATATCCAATTGATTAGTTAAAGCTGCTAATGGTGCT		Ec
CBJP553	HaTAL1	Forward	CATCTTAGTATATTAGTTAAGTATAAGAAGGAGATATACATATGAGCAC CACCCTGATTC		Ec
CBJP554	HaTAL1	Reverse	TGGCCGGCCGATATCCAATTGATTAGGCGAAACAGAATAATACTACGCA		Ec
CBJP555	FjTAL	Forward	CATCTTAGTATATTAGTTAAGTATAAGAAGGAGATATACATATGAACACC ATCAACGAATATCTG		Ec
CBJP556	FjTAL	Reverse	TGGCCGGCCGATATCCAATTGATTAATTGTTAATCAGGTGGTCTTTT ACTTTCTG		Ec
CBJP559	His6-tag	Forward	TATGGCCACCATCATCACCACCATGAGAACCTCTACTTCCA		His
CBJP560	His6-tag	Reverse	GATCTGGAAGTAGAGGTTCTCATGGTGGTGATGGTGGCCA		His
CBJP561	RsTAL	Forward	CACCACCATGAGAACCTCTACTTCCAGATCAGTGATGGTGAGCCCT		His
CBJP562	S_BagA	Forward	CACCACCATGAGAACCTCTACTTCCAGATGAAAATTGATGGTCGTGGTCTG		His
CBJP563	RmXAL	Forward	CACCACCATGAGAACCTCTACTTCCAGATGGCACCGAGCGGTTGATAGC		His
CBJP564	SeSam8	Forward	CACCACCATGAGAACCTCTACTTCCAGATGACCCAGGTTGTTGAACG		His
CBJP565	BlPAL	Forward	CACCACCATGAGAACCTCTACTTCCAGATGAGCCAGGTTGCACTG		His
CBJP566	R_XAL	Forward	CACCACCATGAGAACCTCTACTTCCAGATGCGTAGCGAACAGCTGA		His
CBJP567	PpPAL	Forward	CACCACCATGAGAACCTCTACTTCCAGATGCACGATGATAACACCAGC		His
CBJP568	LbTAL	Forward	CACCACCATGAGAACCTCTACTTCCAGATGCCTCGTTTTTGTCCGA		His
CBJP569	IITAL	Forward	CACCACCATGAGAACCTCTACTTCCAGATGACCACCTCCATTATTGC		His
CBJP570	DdPAL	Forward	CACCACCATGAGAACCTCTACTTCCAGATGATCGAAACCAACCACA		His
CBJP571	SrXAL	Forward	CACCACCATGAGAACCTCTACTTCCAGATGAGCACCCGAGCGCA		His
CBJP572	L_XAL	Forward	CACCACCATGAGAACCTCTACTTCCAGATGACCCTGACCCCGAC		His
CBJP573	HaTAL1	Forward	CACCACCATGAGAACCTCTACTTCCAGATGAGCACCACCCTGATTC		His
CBJP574	FjTAL	Forward	CACCACCATGAGAACCTCTACTTCCAGATGAACACCATCAACGAATATCTG		His

Primer	Target	Direction	Sequence	Host
CBJP575	pCBJ229	Forward	TAATCAATTGGATATCGGCGGCCA	Plasmid amplification
CBJP576	pCBJ229	Reverse	CATCTGGAAGTAGAGGTTCTCATGTGGTG	Plasmid amplification
CBJP637	SeSam8	Forward	ATCTGTCAUAAAACAATGACCCAGGTTGTTGAACG	Sc
CBJP638	SeSam8	Reverse	CACGCGAUTCAGCCAAAATCTTTACCATCTGC	Sc
CBJP645	HaTAL1	Forward	ATCTGTCAUAAAACAATGAGCACCACCCTGATTC	Sc
CBJP646	HaTAL1	Reverse	CACGCGAUTCAGCGAAACAGAATAATACTACGCA	Sc
CBJP647	FjTAL	Forward	ATCTGTCAUAAAACAATGAACACCATCAACGAATATCTG	Sc
CBJP648	FjTAL	Reverse	CACGCGAUTCAATTGTTAATCAGGTGGTCTTTTACTTTCTG	Sc
CBJP649	HaTAL1_Sc	Forward	ATCTGTCAUAAAACAATGTCCACCACCTTGATTTTGA	Sc
CBJP650	HaTAL1_Sc	Reverse	CACGCGAUTCATCTGAACAAGATGATGGATCTCAA	Sc
CBJP651	FjTAL_Sc	Forward	ATCTGTCAUAAAACAATGAACACCATCAACGAATACTTG	Sc
CBJP652	FjTAL_Sc	Reverse	CACGCGAUTCAGTTGTTAATCAAGTGATCCTTAACTTTTTGG	Sc
CBJP741	RtXAL, RtXALmut1-EP18Km-6, RtXALmut2-RM120-1	Forward	CATCTTAGTATATTAGTTAAGTATAAGAAGGAGATATACATATGGCACCGAGCCTGGATAG	Ec
CBJP742	RtXAL, RtXALmut1-EP18Km-6, RtXALmut2-RM120-1	Reverse	TGGCCGGCCGATATCCAATTGATTTAGGCCAGCATTTTCAG	Ec
CBJP743	TcXAL	Forward	CATCTTAGTATATTAGTTAAGTATAAGAAGGAGATATACATATGTTCATCGAAACCAATGTTG	Ec
CBJP744	TcXAL	Reverse	TGGCCGGCCGATATCCAATTGATTTAAAACATTTTACCAACTGCAC	Ec
CBJP745	RcTAL-var1	Forward	CATCTTAGTATATTAGTTAAGTATAAGAAGGAGATATACATATGCTGGATGCAACCATTGG	Ec
CBJP746	RcTAL-var1	Reverse	TGGCCGGCCGATATCCAATTGATTTATGCCGGAGGATCCGCT	Ec
CBJP747	RcTAL-var2	Forward	CATCTTAGTATATTAGTTAAGTATAAGAAGGAGATATACATATGACCCTGCAGAGCCAGAC	Ec
CBJP748	RcTAL-var2 upstream part	Reverse	CGATCAATGGTTTCCGGACT	Ec
CBJP749	RcTAL-var2 middle part	Forward	GTGCAAGTCCGGAAACCATTGATCGTATTGTTGCCGTTCTG	Ec
CBJP750	RcTAL-var2 middle part	Reverse	CGATCACGCAGATCACGTGCGGTCAG	Ec
CBJP752	HaTal2	Forward	CATCTTAGTATATTAGTTAAGTATAAGAAGGAGATATACATATGCGTCATCAGGTTACC	Ec
CBJP753	HaTal2	Reverse	TGGCCGGCCGATATCCAATTGATTTAGGCAAACAGAATAATACTACG	Ec
CBJP754	RtXAL, RtXALmut1-EP18Km-6,RtXALmut2-RM120-1	Forward	ATCTGTCAUAAAACAATGGCACCGAGCCTGGATAG	Sc
CBJP755	RtXAL, RtXALmut1-EP18Km-6,RtXALmut2-RM120-1	Reverse	CACGCGAUTCAGGCCAGCATTTTCAGCA	Sc
CBJP758	RcTAL-var1	Forward	ATCTGTCAUAAAACAATGCTGGATGCAACCATTGG	Sc
CBJP759	RcTAL-var1	Reverse	CACGCGAUTCATGCCGGAGGATCCGCT	Sc
CBJP760	RcTAL-var2	Forward	ATCTGTCAUAAAACAATGACCCTGCAGAGCCAGAC	Sc
CBJP761	RcTAL-var2	Reverse	CACGCGAUTCATGCCAGGGCGGATCTGCG	Sc
CBJP762	HaTAL2	Forward	ATCTGTCAUAAAACAATGCGTCATCAGGTTACC	Sc
CBJP763	HaTAL2	Reverse	CACGCGAUTCAGGCAAACAGAATAATACTACGCAG	Sc
CBJP812	PcXAL	Forward	CATCTTAGTATATTAGTTAAGTATAAGAAGGAGATATACATATGCCGAGCCGTATTGATTATTACAC	Ec
CBJP813	PcXAL	Reverse	TGGCCGGCCGATATCCAATTGATTTAATGCTTTAATGCTTTTCACCAGCA	Ec
CBJP815	PcXAL	Forward	ATCTGTCAUAAAACAATGCCGAGCCGTATTGATTATTACAC	Sc
CBJP816	PcXAL	Reverse	CACGCGAUTCAGGCTTTAATGCTTTTCACCAGCA	Sc
CBJP828	RtXALmut1-EP18Km-6, RtXALmut2-RM120-1	Reverse	TTGCACGCAGATCAATGGCCT	Ec
CBJP829	RtXALmut1-EP18Km-6, RtXALmut2-RM120-1	Forward	CTGCAGGCCATTGATCTGCGTGCAACCGAATTTGAGTTCAAAAAACAGTTTGG	Ec
CBJP830	RtXALmut2-RM120-1	Reverse	TCCAGCAGTGCTTTTCTGCGAGGCTAATTGCACCTTCGGTACGGGTATCTG	Ec
CBJP831	RtXALmut2-RM120-1	Forward	TTAGCCTGCGAAAAGCACTGCTGGAACATCTGCGTGTGTGTTCTGCCGAGCAGCT	Ec
TAL1_fw	RsTAL	Forward	AGTGCAGGUAAAACAATGAGCCCTCCGAAACCGGCAGTTGAACTGG	Sc
TAL1_rv	RsTAL	Reverse	CGTGCGAUTTAAACCGGACTCTGTTG	Sc
TAL2_fw	S_BagA	Forward	AGTGCAGGUAAAACAATGAAAATTGAAAATTGATGGTCGTGGTCTGACCATTAGCCAGACCG	Sc
TAL2_rv	S_BagA	Reverse	CGTGCGAUTTACAGATTACCGCCTGC	Sc
TAL3_fw	RmXAL	Forward	AGTGCAGGUAAAACAATGGCCACCGAGCGTTGATAGC	Sc

TABLE 1 (Continued)

Oligonucleotide	Gene	Direction	Sequence	Restriction site[a]	Use (reference)[b]
TAL3_rv	RmXAL	Reverse	CGTGCGAUTTAGGCCATCATTTTAAC		Sc
TAL4_fw	SeSam8	Forward	AGTGCAGGUAAAACAATGACCCAGGTTGTTGAACGTCAGG		Sc
TAL4_rv	SeSam8	Reverse	CGTGCGAUTTAGCCAAAATCTTTACC		Sc
TAL5_fw	BlPAL	Forward	AGTGCAGGUAAAACAATGAGCCAGGTTGCACTGTTTG		Sc
TAL5_rv	BlPAL	Reverse	CGTGCGAUTTAATCATTCACATTCTG		Sc
TAL6_fw	R_XAL	Forward	AGTGCAGGUAAAACAATGCGTAGCGAACAGCTGACC		Sc
TAL6_rv	R_XAL	Reverse	CGTGCGAUTTAGGCGAGCAGTTCAAT		Sc
TAL7_fw	PpPAL	Forward	AGTGCAGGUAAAACAATGCACGATGATAACACCAGCCCG		Sc
TAL7_rv	PpPAL	Reverse	CGTGCGAUTTAACAGCTTGCGCGTGC		Sc
TAL8_fw	LbTAL	Forward	AGTGCAGGUAAAACAATGCCTCGTTTTGTCCGAGCATGTATCTGC		Sc
TAL8_rv	LbTAL	Reverse	CGTGCGAUTTAATCGTTCGGGGTCAT		Sc
TAL9_fw	IITAL	Forward	AGTGCAGGUAAAACAATGACCACCTCCATTATTGCATTTGG		Sc
TAL9_rv	IITAL	Reverse	CGTGCGAUTTATGCCGGTTCTTGATA		Sc
TAL10_fw	DdPAL	Forward	AGTGCAGGUAAAACAATGATCGAAACCAACCACAAA		Sc
TAL10_rv	DdPAL	Reverse	CGTGCGAUTTACAGGTTCAGGTTAAT		Sc
TAL11_fw	SrXAL	Forward	AGTGCAGGUAAAACAATGAGCACCCCGAGCGCA		Sc
TAL11_rv	SrXAL	Reverse	CGTGCGAUTTATGCGGTCGGAGGGGT		Sc
TAL12_fw	L_XAL	Forward	AGTGCAGGUAAAACAATGACCCTGACCCCGACCG		Sc
TAL12_rv	L_XAL	Reverse	CGTGCGAUTTAGTTAAAGCTGCTAAT		Sc
TAL13_fw	HaTAL1	Forward	AGTGCAGGUAAAACAATGAGGCACCACCCTGATTCTG		Sc
TAL13_rv	HaTAL1	Reverse	CGTGCGAUTTAGGCGAAACAGAATAAT		Sc
TAL14_fw	FjTAL	Forward	AGTGCAGGUAAAACAATGAACACCATCAACGAATATCTGAGC		Sc
TAL14_rv	FjTAL	Reverse	CGTGCGAUTTAATTGTTAATCAGGTG		Sc
PPGK1_fw	PPGK1 promoter	Forward	CGTGCGAUGGAAGTACCTTCAAAGA		Sc (49)
PPGK1_rv	PPGK1 promoter	Reverse	ATGACAGAUTTGTTTTATATTTGTTG		Sc (49)
PTEF1_fw	PTEF1	Forward	ACCTGCACUTGTAATTAAAACTTAG		Sc (49)
PTEF1_rv	PTEF1	Reverse	CACGCGAUGCACACCATAGCTTC		Sc (49)
pIntFwdU	S. cerevisiae chromosomal DNA	Forward	ACCCAAUTCGCCCTATAGTGAGTCG		Sc; integration verification
XI-5 down_out	S. cerevisiae chromosomal DNA	Reverse	CCCAAAAGCAATCCAGGAAAAACC		Sc; integration verification
Pnis_1			GGTGAGTGCCTCCTTATAATTTATTTTG		Ll
Pnis_2			AAGCTTTCTTTGAACCAAAATTAGAAAACC		Ll
TAL_Rs_fw1	RsTALLl	Forward	CAAAATAAATTATAAGGAGGCACTCACCATGCTTGCTATGTCACC ACCAAAACC		Ll
TAL_Rs_rv2	RsTALLl	Reverse	GGTTTTCTAATTTTGGTTCAAAGAAAGCTTTTAAACTGGTGATTGTT GTAATAAATG		Ll
TAL_Rr_fw1	RmXALLl	Forward	CAAAATAAATTATAAGGAGGCACTCACCATGGCTCCATCAGTTGAT TCAATTGC		Ll
TAL_Rr_rv2	RmXALLl	Reverse	GGTTTTCTAATTTTGGTTCAAAGAAAGCTTTTAAGCCATCATTTTAA CTAAAACTGG		Ll
TAL_4_fw1	SeSam8	Forward	CATGTCATGACCCAGGTTGTTGAACG	BspHI	Ll
TAL_4_rv1	SeSam8	Reverse	GCTCTAGATTAGCCAAAATCTTTACCATC	XbaI	Ll
TAL_6_fw1	R_XAL	Forward	GCGGTCTCCCATGCGTAGCGAACAGCTGAC	BsaI	Ll
TAL_6_rv1	R_XAL	Reverse	GCTCTAGATTAGGCCAGCAGTTCAATCAG	XbaI	Ll
TAL_13_fw1	HaTAL1	Forward	GCGGTCTCCCATGAGCACCACCCTGATTCTG	BsaI	Ll
TAL_13_rv1	HaTAL1	Reverse	GCTCTAGATTAGGCGAAACAGAATAATACTACG	XbaI	Ll
TAL_14_fw1	FjTAL	Forward	CATGTCATGAACACCATCAACGAATATC	BspHI	Ll
TAL_14_rv1	FjTAL	Reverse	GCTCTAGATTAATTGTTAATCAGGTGGTC	XbaI	Ll

[a] Underlining indicates restriction sites.
[b] Ec, expression in E. coli; His, His tag; Sc, expression in S. cerevisiae; Ll, expression in L. lactis.

purified. The genes were inserted by isothermal assembly using Gibson Assembly master mix (New England BioLabs), and transformed into chemically competent DH5α (laboratory strain) or NEB5α (New England BioLabs), selecting for resistance to 50 μg ml^{-1} spectinomycin in LB medium. A few genes were constructed by assembly of multiple fragments: the gene encoding RsTAL-var2 was assembled from two fragments PCR amplified from the gene encoding RcTAL-var1 and the synthetic double-stranded DNA fragment CBJBB6 (see Table S1 in the supplemental material). The genes encoding RtXAL-EP18Km-6 and RtPALmut2-RM120-1 were constructed by assembly of two and three, respectively, PCR products amplified from the gene encoding RtXal1. Plasmids carrying genes encoding His-tagged versions of the proteins were made as follows. Partly complementary oligonucleotides CBJP559 and CBJP560 were ligated into pCDFDuet-1 digested with NdeI and BglII, forming a new histidine tag. The resulting plasmid pCBJ229 was PCR amplified with CBJP575 and CBJP576, and this linear DNA fragment was combined with individual genes amplified with the oligonucleotides shown in Table 1 as described previously. Clones were verified by sequencing and electroporated into the *E. coli* expression strain BL21(DE3)/pLysS (Invitrogen/Life Technologies), selecting for pLysS with 34 μg ml^{-1} chloramphenicol and for expression plasmids with 50 μg ml^{-1} spectinomycin. A control strain carrying pCDFDuet-1 was also made. The resulting plasmids and strains are shown in Tables 2 and 3, respectively.

(iv) Cloning for expression in *Saccharomyces cerevisiae*. All genetic constructions were made in *E. coli* DH5α grown in LB containing 100 μg ml^{-1} ampicillin for plasmid maintenance. Fourteen of the genes cloned for expression in *E. coli* and the TEF1 promoter were amplified using the uracil-containing primers listed in Table 1. The promoter fragment and each of the genes were combined into the integrative EasyClone vector, pCfB391 (49) following the uracil-specific excision reagent (USER) cloning method (54). The resulting plasmids are listed in Table 2. Plasmids were digested by NotI and purified by using NucleoSpin gel and PCR cleanup kits (Macherey-Nagel) following manual instructions. DNA linearized plasmids (300 to 700 ng) were transformed into *S. cerevisiae* CEN.PK102-5B (*MAT**a** ura3-52 his3Δ1 leu2-3/112 MAL2-8c SUC2*) by the lithium acetate transformation protocol (55). Yeast transformants were selected on synthetic complete (SC) dropout medium without histidine, resulting in strains STC0 to STC14. Correct insertions of TAL genes were verified by yeast colony PCR by primers pIntFwdU and XI-5 down_out. Alternatively, for plasmid-borne expression, 12 genes, including those encoding HaTAL1 and FjTAL optimized for *S. cerevisiae* (see Table S1 in the supplemental material), were amplified using the oligonucleotide also listed in Table 1 and inserted by uracil excision into the vector pCfB132 together with the PPGK1 promoter amplified by primers PPGK1_fw and PPGK1_rv (49). The finished plasmids were transformed into *S. cerevisiae* CEN.PK102-5B selecting for growth on synthetic dropout medium plates lacking uracil. Control strains with either the integration of pCfB391 or carrying pCfB1322 were also made. The resulting plasmids and strains are shown in Tables 2 and 3, respectively.

(v) Cloning for expression in *Lactococcus lactis*. The synthetic RsTAL$_{LL}$ and RmXAL$_{LL}$ genes (see Table S1 in the supplemental material) were cloned into the nisin-inducible expression vector pNZ8048 (56) as follows. RsTAL$_{LL}$ and RmXAL$_{LL}$ genes and the vector were PCR amplified using the primers listed in Table 1 and assembled in a single-tube isothermal reaction using the Gibson Assembly master mix (New England BioLabs). Reaction products were ethanol precipitated and suspended in double-distilled water before transformation into *L. lactis* by electroporation as described by Holo and Nes (57). The synthetic genes encoding SeSam8, R_XAL, HaTAL1, and FjTAL were amplified by PCR using the primer pairs listed in Table 1, digested with specific restriction enzymes, and cloned between the NcoI and XbaI restriction sites of pNZ8048. The plasmids were obtained and maintained in NZ9000 (56), and the gene sequences of the different constructs were verified by sequencing. To assess pHCA production, TAL expression vectors were transformed into NZ9000Δ*ldh*Δ*ldhB* (86). A control strain was also constructed by trans-

formation of NZ9000Δ*ldh*Δ*ldhB* with empty expression vector pNZ8048. Plasmids and strains are listed in Tables 2 and 3.

Analysis of production. (i) Heterologous TAL and PAL expression and analysis of pHCA and CA production in *E. coli*. Unless otherwise stated, pHCA production was carried out as follows. *E. coli* BL21(DE3) pLysS strains harboring recombinant plasmids were precultured in 3 ml of 2×YT with appropriate antibiotics and incubated at 37°C and 250 rpm overnight. The following day, each preculture was transferred into 2 ml of M9 minimal medium with appropriate antibiotics to a final OD$_{600}$ of 0.05 and cultured at 37°C and 300 rpm in 24-well deep-well plates (Enzyscreen B.V., Netherlands) until the OD$_{600}$ reached ~0.6. Then, isopropyl β-D-1 thiogalactopyranoside (IPTG) was added at a final concentration of 1 mM, and the cells were grown for 3 h at 30°C, followed by addition of 2 mM substrate (tyrosine, phenylalanine, or histidine). Finally, the culture was incubated at 30°C for 24 h. In the case of the time course experiments with *E. coli*, samples were collected every hour for 14 h and after 24 h from substrate addition. Collected samples were harvested by centrifugation at 16,200 × *g* for 10 min, and the supernatant was filtered through 0.2-μm filters and analyzed by using high-performance liquid chromatography (HPLC) as described below. Experiments were carried out at least in triplicate.

(ii) Heterologous TAL and PAL expression and analysis of pHCA and CA production in *S. cerevisiae*. For screening the 14 different chromosomally integrated TAL and PAL genes, yeast cultures were grown in 0.5 ml SC medium lacking histidine at 30°C and 250 rpm for 24 h in a 96-well deep-well plate, and then 50 μl of this preculture was inoculated into 0.5 ml Delft medium with 2% glucose or into FIT medium, both of which were supplemented with 76 mg liter^{-1} uracil, 380 mg liter^{-1} leucine, and 10 mM tyrosine or phenylalanine. Yeast cultures were cultivated in 96-well deep-well plates at 30°C and 250 rpm for 72 h. Samples for HPLC were taken at the endpoint of cultivation, and the OD$_{600}$ of the yeast cultures was measured in a microtiter plate reader after cultures had been diluted 2 to 20 times. A similar procedure was used for the analysis of strains carrying genes on episomal plasmids, except that selection was done in medium without uracil.

(iii) Heterologous TAL and PAL expression and analysis of pHCA and CA production in *L. lactis*. For heterologous expression of cloned tyrosine ammonia-lyases, *L. lactis* strains were grown in CDM, and nisin (1.5 μg liter^{-1}) was added at an OD$_{600}$ of 0.3 to 0.4. Samples (1 ml) of cultures were collected at different points during growth and centrifuged (16,100 × *g*, 10 min, 4°C), and the supernatants were stored at −20°C until analysis by HPLC.

Analytical methods. The production of pHCA, cinnamic acid, and urocanic acid was measured by HPLC on a Thermo HPLC setup and quantified using standards (Sigma-Aldrich). Samples were analyzed by a gradient method with two solvents: 10 mM ammonium formate (pH 3.0) (A) and acetonitrile (B) at 1.5 ml min^{-1}, starting at 5% B. From 0.5 min after injection to 7 min, the fraction of B increased linearly from 5% to 60%, and between 9.5 and 9.6 min, the fraction of B decreased back to 5%, remaining there until 12 min. pHCA and CA were quantified by measuring absorbance at 333 nm and 277 nm, respectively. Titers were calculated by correlating OD$_{600}$ to grams (dry weight) of cells (CDW) liter^{-1}, using previously measured correlation or literature values (58, 59).

Protein purification and kinetic analysis. Strains expressing His-tagged versions of the enzymes were grown in LB medium overnight at 37°C, diluted into fresh LB with 1 mM IPTG, and propagated overnight (approximately 18 h) at 30°C. Cells were harvested by centrifugation at 9,800 × *g* for 8 min and disrupted using an EmulsiFlex-C5 homogenizer (Avestin) into a buffer (50 mM Tris-HCl, 10 mM imidazole, 500 mM NaCl, 10% glycerol [pH 7.5]). The supernatant was clarified by centrifugation at 10,000 × *g* for 10 min at 4°C and loaded onto nickel-nitrilotriacetic acid (Ni^{2+}-NTA) resin columns on an Äkta Pure system connected to an F9-C fraction collector (GE). Finally, the fractions containing the purified protein was dialyzed overnight against a buffer containing 50 mM Tris-HCl (pH 7.5), 150 mM NaCl, and 10% glycerol, flash-frozen in liquid

TABLE 2 Plasmids

Name	Parent vector	Description[a]	Source or reference
pCDFDuet-1			Novagen
pCBJ215	pCDFDuet-1	pCDFDuet-1 MCS2::RsTAL, Sp[r]	This work
pCBJ216	pCDFDuet-1	pCDFDuet-1 MCS2::S_BagA, Sp[r]	This work
pCBJ217	pCDFDuet-1	pCDFDuet-1 MCS2::RmXAL, Sp[r]	This work
pCBJ218	pCDFDuet-1	pCDFDuet-1 MCS2::SeSam8, Sp[r]	This work
pCBJ219	pCDFDuet-1	pCDFDuet-1 MCS2::BlPAL, Sp[r]	This work
pCBJ220	pCDFDuet-1	pCDFDuet-1 MCS2::R_XAL, Sp[r]	This work
pCBJ221	pCDFDuet-1	pCDFDuet-1 MCS2::PpPAL, Sp[r]	This work
pCBJ222	pCDFDuet-1	pCDFDuet-1 MCS2::LbTAL, Sp[r]	This work
pCBJ223	pCDFDuet-1	pCDFDuet-1 MCS2::IlTAL, Sp[r]	This work
pCBJ224	pCDFDuet-1	pCDFDuet-1 MCS2::DdPAL, Sp[r]	This work
pCBJ225	pCDFDuet-1	pCDFDuet-1 MCS2::SrXAL, Sp[r]	This work
pCBJ226	pCDFDuet-1	pCDFDuet-1 MCS2::L_XAL, Sp[r]	This work
pCBJ227	pCDFDuet-1	pCDFDuet-1 MCS2::HaTAL1, Sp[r]	This work
pCBJ228	pCDFDuet-1	pCDFDuet-1 MCS2::FjTAL, Sp[r]	This work
pCBJ229	pCDFDuet-1	pCDFDuet-1-His6; cloning vector for expression of His$_6$-tagged proteins, Sp[r]	This work
pCBJ230	pCBJ229	pCBJ229::RsTAL, Sp[r]	This work
pCBJ233	pCBJ229	pCBJ229::SeSam8, Sp[r]	This work
pCBJ242	pCBJ229	pCBJ229::HaTAL1, Sp[r]	This work
pCBJ243	pCBJ229	pCBJ229::FjTAL, Sp[r]	This work
pCfB132		Episomal replication vector with USER cassette derived from pESC-URA (Agilent); Amp[r], URA	49
pCBJ278	pCfB132	pCfB132::PPGK1->SeSam8, Amp[r], URA	This work
pCBJ279	pCfB132	pCfB132::PPGK1->HaTAL1, Amp[r], URA	This work
pCBJ280	pCfB132	pCfB132::PPGK1->FjTAL, Amp[r], URA	This work
pCBJ281	pCfB132	pCfB132::PPGK1->HaTAL1Sc, Amp[r], URA	This work
pCBJ282	pCfB132	pCfB132::PPGK1->FjTALSc, Amp[r], URA	This work
pCBJ295	pCDFDuet-1	pCDFDuet-1 MCS2::RtXAL, Sp[r]	This work
pCBJ296	pCDFDuet-1	pCDFDuet-1 MCS2::TcXAL, Sp[r]	This work
pCBJ297	pCDFDuet-1	pCDFDuet-1 MCS2::RcTAL-var1, Sp[r]	This work
pCBJ298	pCDFDuet-1	pCDFDuet-1 MCS2::RcTAL-var2, Sp[r]	This work
pCBJ299	pCDFDuet-1	pCDFDuet-1 MCS2::HaTAL2, Sp[r]	This work
pCBJ300	pCDFDuet-1	pCDFDuet-1 MCS2::PcXAL, Sp[r]	This work
pCBJ301	pCDFDuet-1	pCDFDuet-1 MCS2::RtXAL-EP18Km-6, Sp[r]	This work
pCBJ302	pCDFDuet-1	pCDFDuet-1 MCS2::RtXAL-RM120-1, Sp[r]	This work
pCBJ303	pCfB132	pCfB132::PPGK1->RtXAL, Amp[r], URA	This work
pCBJ304	pCfB132	pCfB132::PPGK1->RcTAL-var1, Amp[r], URA	This work
pCBJ305	pCfB132	pCfB132::PPGK1->RcTAL-var2, Amp[r], URA	This work
pCBJ306	pCfB132	pCfB132::PPGK1->HaTAL2, Amp[r], URA	This work
pCBJ307	pCfB132	pCfB132::PPGK1->PcXAL, Amp[r], URA	This work
pCBJ308	pCfB132	pCfB132::PPGK1->RtXAL-EP18Km-6, Amp[r], URA	This work
pCBJ309	pCfB132	pCfB132::PPGK1->RtXAL-RM120-1, Amp[r], URA	This work
pCfB391		pXI-5-HIS5, yeast integrative plasmid containing USER cassette; TADH1 and TCYC1 from *S. cerevisiae*, Amp[r]	49
pCfB860	pCfB391 (pXI-5-HIS5)	RsTAL, Amp[r], HIS	This work
pCfB861	pCfB391 (pXI-5-HIS5)	S_BagA, Amp[r], HIS	This work
pCfB862	pCfB391 (pXI-5-HIS5)	RmXAL, Amp[r], HIS	This work
pCfB863	pCfB391 (pXI-5-HIS5)	SeSam8, Amp[r], HIS	This work
pCfB864	pCfB391 (pXI-5-HIS5)	BlPAL, Amp[r], HIS	This work
pCfB865	pCfB391 (pXI-5-HIS5)	R_XAL, Amp[r], HIS	This work
pCfB866	pCfB391 (pXI-5-HIS5)	PpPAL, Amp[r], HIS	This work
pCfB867	pCfB391 (pXI-5-HIS5)	LbTAL, Amp[r], HIS	This work
pCfB868	pCfB391 (pXI-5-HIS5)	IlTAL, Amp[r], HIS	This work
pCfB869	pCfB391 (pXI-5-HIS5)	DdPAL, Amp[r], HIS	This work
pCfB870	pCfB391 (pXI-5-HIS5)	SrXAL, Amp[r], HIS	This work
pCfB871	pCfB391 (pXI-5-HIS5)	L_XAL, Amp[r], HIS	This work
pCfB872	pCfB391 (pXI-5-HIS5)	HaTAL1, Amp[r], HIS	This work
pCfB873	pCfB391 (pXI-5-HIS5)	FjTAL, Amp[r], HIS	This work
pNZ8048		Cm[r]; inducible expression vector carrying P$_{nisA}$	56
pNZ_RsTAL$_{Ll}$	pNZ8048	Cm[r]; derivative of pNZ8048 carrying the *Rhodobacter sphaeroides* TAL-encoding gene codon optimized for expression in *L. lactis*	Gaspar et al., unpublished

(Continued on following page)

TABLE 2 (Continued)

Name	Parent vector	Description[a]	Source or reference
pNZ_RmXAL$_{Ll}$	pNZ8048	Cm^r; derivative of pNZ8048 carrying the *Rhodotorula mucilaginosa* PAL/TAL-encoding gene codon optimized for expression in *L. lactis*	This work
pNZ_SeSam8	pNZ8048	Cm^r; derivative of pNZ8048 carrying the SeSam8-encoding gene codon optimized for expression in *E. coli*	This work
pNZ_R_XAL	pNZ8048	Cm^r; derivative of pNZ8048 carrying the R_XAL-encoding gene codon optimized for expression in *E. coli*	This work
pNZ_HaTAL1	pNZ8048	Cm^r; derivative of pNZ8048 carrying the HaTAL1-encoding gene codon optimized for expression in *E. coli*	This work
pNZ_FjTAL	pNZ8048	Cm^r; derivative of pNZ8048 carrying the FjTAL-encoding gene codon optimized for expression in *E. coli*	This work

[a] Cm^r, chloramphenicol resistance; Sp^r, spectinomycin resistance; Amp^r, ampicillin resistance.

nitrogen, and stored at −80°C. The purification and protein sizes were assessed by SDS-PAGE (see Fig. S2 in the supplemental material).

Enzymatic assays were performed in 200-μl volumes in wells in a UV transparent 96-well plate, by following the increase in absorbance at 315 nm (pHCA) or 295 nm (CA). The pH optima were determined in 50 mM potassium phosphate buffer for pH 6.0 to 8.0 and in 50 mM potassium borate buffer for pH 8.5 to 10.5. The reaction mixtures contained 2 μg of purified protein, and the reactions were initiated with 1 mM tyrosine or 6 mM phenylalanine after equilibration to 30°C. The enzymatic activity was expressed in units per gram, where 1 unit is defined as 1 μmol substrate converted per minute. We did not observe any production in the absence of enzymes under any conditions.

The kinetic constants K_m and V_{max} were determined from assays containing from 1.56 μM to 200 μM tyrosine or from 193 μM to 25 mM phenylalanine.

Nucleotide sequence accession numbers. The codon-optimized genes (see Table S1 in the supplemental material) have been deposited in GenBank under accession numbers KR095285 to KR095310.

RESULTS AND DISCUSSION

Using synteny and phylogeny to identify enzymes. We examined the diversity of known and hypothetical XAL enzymes, aiming at identifying enzymes from the protein sequence databases that differed from the previously characterized enzymes. For this purpose, we created a protein sequence subset from the nonredundant protein sequence database at GenBank by identifying homologs to four nonsimilar known genes with TAL or PAL activity: those encoding RsTAL from *R. sphaeroides* (1, 60), S_BagA from *Streptomyces* (40), RmXAL from *Rhodotorula mucilaginosa* (61, 62), and SeSam8 from *Saccharothrix espanaensis* (21, 63).

In order to assess the true diversity of XAL enzymes, and to further counter the challenge of sequence bias, we condensed the data set for 4,729 unique sequences into 107 representative clusters, each containing 1 to 1,201 sequences with more than 40% sequence identity to the first cluster representative sequence.

Sequencing bias is illustrated by the fact that 99% of sequences found in the largest cluster, making up one fourth of all sequences, could be identified as belonging to proteobacteria. To a large extent, each cluster represented sequences found in a single phylum, but a single phylum could be represented in several clusters. For example, a single strain may have two homologs in its genome, one being a HAL and the other a PAL. Overall, the majority of sequences were of bacterial origin, with proteobacteria contributing to 47% of all sequences that could be assigned to phyla, reflecting the overrepresentation of proteobacteria in the database.

Figure 2 shows a phylogenetic tree containing representatives of each cluster together with previously characterized proteins

(see Table S2 in the supplemental material) (all functionally characterized TAMs, PAMs, and TALs listed in BRENDA [http://www.brenda-enzymes.info] [64], 10 PALs, and three HALs) and enzymes chosen for further study here.

Since functionally related genes may show synteny (colocalization of genetic loci) and cluster together (high linkage) in microbial genomes, we examined the combinatorial presence of characteristic proteins that could hint at the activity encoded by the candidate gene. Some bacteria use pHCA as a chromophore in the light-sensing photoactive yellow protein (PYP) (18, 65), and homologs to PYP were found in close proximity to a TAL homolog in *Idiomarina loihiensis*, *Halorhodospira halophila*, and *Curvibacter*. *R. sphaeroides*, *Rhodobacter capsulatus*, *Salinibacter ruber* (66), *Rhodopseudomonas palustris*, *Sorangium cellulosum*, *Leptospira biflexa*, *Leptothrix cholodnii*, *Gemmatimonas aurantiaca*, and *Haliangium ochraceum* carry PYP gene homologs elsewhere in their chromosomes, while other bacteria (*Rhodospirillum centenum*, *Methylobacterium extorquens*, *Methylobacterium* sp. strain 4-46, *Methylobacterium radiotolerans*, *Methylobacterium populi*, and *Methylobacterium chloromethanicum*) have a PYP homolog as part of a larger protein.

The enzyme 4-coumaroyl-CoA ligase (4CL) forms the activated thioester from pHCA and CoA, required for example for formation of pHCA-bound PYP or for formation of flavonoids or stilbenes. A homolog to a 4CL may act on either pHCA or CA, but not on urocanic acid, and is thus linked to PAL and TAL activity but not HAL activity. HAL activity is the first step in the degradation of histidine to urocanic acid, which is then processed by the enzyme urocanase (urocanate hydratase), whose gene is commonly annotated as *hutU* in bacteria.

Thus, we used linkage (within a distance of five genes) of either a 4CL gene or *hutU* as a criterion for predicting enzymatic function, and the clusters containing XAL homologs closely linked to 4CL or *hutU* are shown in Fig. 2. No cluster contained two XALs with different linkages. The largest clusters carried sequences homologous to HALs and linkage to *hutU*, showing that the HAL functionality is more abundant in the sequence database (Table 4). However, close inspection showed that, the catalytically important MIO-forming amino acid triad and a conserved tyrosine (Y300 in RsTAL) (22) were absent from many sequences, while the immediate surrounding amino acid residues were conserved. Some of the coding sequences are genetically linked to histidine degradative genes, and it is unclear if their products are catalytically active as histidases independent of a MIO-based mechanism, e.g., by using an alternative prosthetic group, such as formation of

TABLE 3 Strains

Strain	Description	Reference or source
E. coli		
CBJ772	DH5α/pCBJ215	This work
CBJ773	DH5α/pCBJ216	This work
CBJ774	DH5α/pCBJ217	This work
CBJ775	NEB5α/pCBJ218	This work
CBJ776	NEB5α/pCBJ219	This work
CBJ777	NEB5α/pCBJ220	This work
CBJ778	NEB5α/pCBJ221	This work
CBJ779	NEB5α/pCBJ222	This work
CBJ780	NEB5α/pCBJ223	This work
CBJ781	NEB5α/pCBJ224	This work
CBJ782	NEB5α/pCBJ225	This work
CBJ783	NEB5α/pCBJ226	This work
CBJ784	NEB5α/pCBJ227	This work
CBJ785	NEB5α/pCBJ228	This work
CBJ786	BL21(DE3)/pLysS pCDFDuet-1	This work
CBJ787	BL21(DE3)/pLysS pCBJ215	This work
CBJ788	BL21(DE3)/pLysS pCBJ216	This work
CBJ789	BL21(DE3)/pLysS pCBJ217	This work
CBJ790	BL21(DE3)/pLysS pCBJ218	This work
CBJ791	BL21(DE3)/pLysS pCBJ219	This work
CBJ792	BL21(DE3)/pLysS pCBJ220	This work
CBJ793	BL21(DE3)/pLysS pCBJ221	This work
CBJ794	BL21(DE3)/pLysS pCBJ222	This work
CBJ795	BL21(DE3)/pLysS pCBJ223	This work
CBJ796	BL21(DE3)/pLysS pCBJ224	This work
CBJ797	BL21(DE3)/pLysS pCBJ225	This work
CBJ798	BL21(DE3)/pLysS pCBJ226	This work
CBJ799	BL21(DE3)/pLysS pCBJ227	This work
CBJ800	BL21(DE3)/pLysS pCBJ228	This work
CBJ801	NEB5α/pCBJ229	This work
CBJ802	NEB5α/pCBJ230	This work
CBJ805	NEB5α/pCBJ233	This work
CBJ814	NEB5α/pCBJ242	This work
CBJ815	NEB5α/pCBJ243	This work
CBJ827	BL21(DE3)/pLysS pCBJ229	This work
CBJ828	BL21(DE3)/pLysS pCBJ230	This work
CBJ831	BL21(DE3)/pLysS pCBJ233	This work
CBJ840	BL21(DE3)/pLysS pCBJ242	This work
CBJ841	BL21(DE3)/pLysS pCBJ243	This work
CBJ889	NEB5α/pCBJ278	This work
CBJ890	NEB5α/pCBJ279	This work
CBJ891	NEB5α/pCBJ280	This work
CBJ892	NEB5α/pCBJ281	This work
CBJ893	NEB5α/pCBJ282	This work
CBJ938	NEB5α/pCBJ295	This work
CBJ939	NEB5α/pCBJ296	This work
CBJ940	NEB5α/pCBJ297	This work
CBJ941	NEB5α/pCBJ298	This work
CBJ942	NEB5α/pCBJ299	This work
CBJ943	NEB5α/pCBJ300	This work
CBJ944	NEB5α/pCBJ301	This work
CBJ945	NEB5α/pCBJ302	This work
CBJ946	BL21(DE3)/pLysS pCBJ295	This work
CBJ947	BL21(DE3)/pLysS pCBJ296	This work
CBJ948	BL21(DE3)/pLysS pCBJ297	This work
CBJ949	BL21(DE3)/pLysS pCBJ298	This work
CBJ950	BL21(DE3)/pLysS pCBJ299	This work
CBJ951	BL21(DE3)/pLysS pCBJ300	This work
CBJ952	BL21(DE3)/pLysS pCBJ301	This work
CBJ953	BL21(DE3)/pLysS pCBJ302	This work
CBJ962	NEB5α/pCBJ303	This work

TABLE 3 (Continued)

Strain	Description	Reference or source
CBJ963	NEB5α/pCBJ304	This work
CBJ964	NEB5α/pCBJ305	This work
CBJ965	NEB5α/pCBJ306	This work
CBJ966	NEB5α/pCBJ307	This work
CBJ967	NEB5α/pCBJ308	This work
CBJ968	NEB5α/pCBJ309	This work
S. cerevisiae		
CEN.PK102-5B	MAT**a** *ura3-52 his3Δ1 leu2-3/112 MAL2-8^c SUC2*	Verena Siewers (Chalmers University)
STC0	Integration of pCfB391 into CEN.PK102-5B	This work
STC1	Integration of pCfB860 into CEN.PK102-5B	This work
STC2	Integration of pCfB861 into CEN.PK102-5B	This work
STC3	Integration of pCfB862 into CEN.PK102-5B	This work
STC4	Integration of pCfB863 into CEN.PK102-5B	This work
STC5	Integration of pCfB864 into CEN.PK102-5B	This work
STC6	Integration of pCfB865 into CEN.PK102-5B	This work
STC7	Integration of pCfB866 into CEN.PK102-5B	This work
STC8	Integration of pCfB867 into CEN.PK102-5B	This work
STC9	Integration of pCfB868 into CEN.PK102-5B	This work
STC10	Integration of pCfB869 into CEN.PK102-5B	This work
STC11	Integration of pCfB870 into CEN.PK102-5B	This work
STC12	Integration of pCfB871 into CEN.PK102-5B	This work
STC13	Integration of pCfB872 into CEN.PK102-5B	This work
STC14	Integration of pCfB873 into CEN.PK102-5B	This work
CBJ969	CEN.PK102-5B/pCBJ278	This work
CBJ970	CEN.PK102-5B/pCBJ279	This work
CBJ971	CEN.PK102-5B/pCBJ280	This work
CBJ972	CEN.PK102-5B/pCBJ281	This work
CBJ973	CEN.PK102-5B/pCBJ282	This work
CBJ981	CEN.PK102-5B/pCfB132	This work
CBJ982	CEN.PK102-5B/pCBJ303	This work
CBJ983	CEN.PK102-5B/pCBJ304	This work
CBJ984	CEN.PK102-5B/pCBJ305	This work
CBJ985	CEN.PK102-5B/pCBJ306	This work
CBJ986	CEN.PK102-5B/pCBJ307	This work
CBJ987	CEN.PK102-5B/pCBJ308	This work
CBJ988	CEN.PK102-5B/pCBJ309	This work
L. lactis		
NZ9000	MG1363 *pepN::nisRK*	56
NZ9000Δ*ldh*Δ*ldhB*	NZ9000 derivative containing the double deletion of *ldh* and *ldhB*	86
NZ9000Δ*ldh*Δ*ldhB* pNZ	NZ9000 Δ*ldh*Δ*ldhB*/pNZ8048	This work
NZ9000Δ*ldh*Δ*ldhB*_RsTAL_{LI}	NZ9000 Δ*ldh*Δ*ldhB*/pNZ_RsTAL_{LI}	This work
NZ9000Δ*ldh*Δ*ldhB*_RmXAL_{LI}	NZ9000 Δ*ldh*Δ*ldhB*/pNZ_RmXAL_{LI}	This work
NZ9000Δ*ldh*Δ*ldhB*_SeSam8	NZ9000 Δ*ldh*Δ*ldhB*/pNZ_SeSam8	This work
NZ9000Δ*ldh*Δ*ldhB*_R_XAL	NZ9000 Δ*ldh*Δ*ldhB*/pNZ_R_XAL	This work
NZ9000Δ*ldh*Δ*ldhB*_HaTAL1	NZ9000 Δ*ldh*Δ*ldhB*/pNZ_HaTAL1	This work
NZ9000Δ*ldh*Δ*ldhB*_FjTAL	NZ9000 Δ*ldh*Δ*ldhB*/pNZ_FjTAL	This work

dehydroalanine, as first suggested for aromatic amino acid ammonia-lyases (15, 67, 68), or if they catalyze an alternative reaction.

From Fig. 2 it is evident that there are large groups of potential enzymes which do not show a high degree of homology to enzymes that have been functionally characterized, while many previously characterized enzymes cluster together. It is also clear that there are large groups of enzymes for which no representative has hitherto been characterized. The known HALs as well as the *hutU*-linked genes from both eukaryotes and prokaryotes form a large group, which is separated from the enzymes that have TAM, PAM, TAL, or PAL activity. This was also found to be true in the cases where a PAL and a HAL are from the same organism.

Aiming at functionally characterizing a wide spectrum of PAL and TAL enzymes, we chose to examine 22 proteins (Table 5), of which half were uncharacterized, representing different clusters. We included two near-identical TALs from *R. capsulatus* (18), a TAL from *R. sphaeroides* (1, 22, 26, 28, 60, 69) which is highly similar with regard to primary sequence (51% amino acid identity) and enzyme kinetics, and a third representative from this cluster (cluster 53), R_XAL, from *Rheinheimera* sp. strain A13L. Two homologs, from the extreme halophilic bacterium *Salinibacter ruber* and from the spirochete *Leptospira biflexa*, grouped with the previously characterized SeSam8 from *Saccharothrix espanaensis* (21). Because the sequences contain active-site residues similar to those

FIG 2 Phylogenetic relationship between enzymes of aromatic amino acid ammonia-lyase homologs. Included are representative from clusters of sequences that are at least 40% identical (after iteration of similar clustering based on 90% and 60% identities) and enzymes with known PAL, TAL, HAL, PAM, and TAM functions. The number of sequences in each cluster is indicated by the number after the vertical line. Characterized enzymes are shown using the following color code: red, PAL; blue, TAL; purple, PAL/TAL; yellow, HAL; light red, PAM; light blue, TAM; white, no activity. Enzymes subject to analysis in this study are marked by circles, while enzymes with activity shown elsewhere in the literature are marked by square symbols. Some groups of enzymes did not carry the sequences required for the formation of the 3,5-dihydro-5-methylidene-4H-imidazol-4-one (MIO) prosthetic group.

of TALs (23), and since the chromosomes furthermore encode PYP homologs, they were predicted to be TALs and included in this study (SrXAL, LbTAL, and SeSam8). The *Idiomarina loihiensis* genome encodes the homolog IlTAL, as well as both a PYP and

a 4CL. BagA from *Streptomyces* sp. showed the greatest homology to BlPAL from the Gram-positive organism *Brevibacillus laterosporus*.

We selected PpPAL from the biotechnologically relevant moss

TABLE 4 The 15 largest sequence clusters and phylogeny of selected TAL genes

Order of cluster size	Size	Top phylum(a) (%)[a]	Linkage within cluster[b]	Enzyme(s) investigated
1	1,201	*Proteobacteria* (99)	*hutU*	
2	763	*Firmicutes* (59), *Bacteroidetes* (24)	*hutU*	
3	504	*Streptophyta* (100)		PpPAL
4	410	*Proteobacteria* (99)	4CL	IlTAL
5	360	*Actinobacteria* (98)	*hutU*	
6	257	*Proteobacteria* (100)	*hutU*	
7	170	*Chordata* (75), *Proteobacteria* (3)	*hutU*	
8	96	*Bacteroidetes* (100)		FjTAL
9	81	*Bacteroidetes* (83), *Proteobacteria* (16)	*hutU*	
10	74	*Actinobacteria* (100)	*hutU*	
11	47	*Euryarchaeota* (98)	*hutU*	
12	42	*Actinobacteria* (68), *Proteobacteria* (32)	4CL	RsTAL, RcTAL, R_XAL
13	41	*Basidiomycota* (100)		PcXAL
14	41	*Proteobacteria* (93)	*hutU*	
15	40	*Firmicutes* (60), *Proteobacteria* (20)	*hutU*	
26-27	16	*Actinobacteria* (75), *Firmicutes* (19)		S_BagA, BlPAL
28-29	15	*Cyanobacteria* (67), *Proteobacteria* (13)		HaTAL, L_XAL
39–42	7	*Basidiomycota* (100)		RmXAL, RtXAL, TcXAL
39–42	7	*Proteobacteria* (100)		DdPAL
39–42	7	*Actinobacteria* (100)		SeSam8
44–50	6	*Spirochaetes* (100)		LbTAL
56–66	3	*Bacteroidetes* (100)		SrXAL

[a] Percentages of sequences that could be assigned to a phylum are shown. Most sequences within a cluster could be assigned to a primary phylum, and in case of less than 90% assignment, the second most represented phylum is shown as well. The largest clusters are formed by bacterial sequences that are generally linked to *hutU* sequences.

[b] Three of the selected enzymes used in this study originate from three large bacterial clusters with no linkage to *hutU*, and there was linkage to 4CL for IlTAL and RsTAL within the cluster, this was not the case for FjTAL.

Physcomitrella patens subsp. *patens*, and the fungal enzymes of RmXAL, TcXAL (25), PcXAL (70), and RtXAL, including two mutants of the latter for which improved enzymatic characteristics have been reported (17, 71). A cyanobacterial sequence from *Leptolyngbya* was chosen together with two other sequences from the genome of the green nonsulfur bacterium (*Chloroflexi*) *Herpetosiphon aurantiacus*. Interestingly, the organism has a third homolog (31% to 32% identity over 474 to 503 amino acids) in its

TABLE 5 Enzymes analyzed in this study

ID	Organism	Protein GI	Length[a]
RmXAL[b]	*Rhodotorula mucilaginosa* (*Rhodotorula rubra*)	129592	713
TcXAL[b]	*Trichosporon cutaneum*	77375521	552
PcXAL[b]	*Phanerochaete chrysosporium*	259279291	506
RtXAL[b]	*Rhodosporidium toruloides*	129593	567
RtXALmut1-EP18Km-6[b]	*Rhodosporidium toruloides*	21503942	567
RtXALmut2-RM120-1[b]	*Rhodosporidium toruloides*	29719264	552
RcTAL-var1[b]	*Rhodobacter capsulatus*	155708849	506
RcTAL-var2[b]	*Rhodobacter capsulatus*	534410416	567
RsTAL[b]	*Rhodobacter sphaeroides*	126464011	523
S_BagA[b]	*Streptomyces*	359308109	529
SeSam8[b]	*Saccharothrix espanaensis*	433607630	510
PpPAL[c]	*Physcomitrella patens* subsp. *patens*	168011366	714
DdPAL[c]	*Dictyostelium discoideum*	66822311	529
BlPAL[c]	*Brevibacillus laterosporus*	339009660	550
R_XAL[c]	*Rheinheimera*	336316228	516
IlTAL[c]	*Idiomarina loihiensis*	56459245	515
LbTAL[c]	*Leptospira biflexa* serovar patoc	183220142	514
L_XAL[c]	*Leptolyngbya*	427415639	567
SrXAL[c]	*Salinibacter ruber*	83816043	517
FjTAL[c]	*Flavobacterium johnsoniae*	146298870	506
HaTAL1[c]	*Herpetosiphon aurantiacus*	159898407	552
HaTAL2[c]	*Herpetosiphon aurantiacus*	159898927	552

[a] Protein length in amino acids.
[b] Previously characterized enzyme.
[c] Novel enzyme included in this study.

genome, which clusters together with the HALs (cluster 43). We furthermore chose to include DdPAL from *Dictyostelium discoideum* as a representative of a rare protein from an amoeba.

Finally, we included a bacterial sequence that showed little similarity to other known enzymes, FjTAL from *Flavobacterium johnsoniae*. This clusters with enzymes from *Bacteroides* but is otherwise grouped most closely to previously described PALs, TAMs, and PAMs mainly from actinobacteria and proteobacteria (Fig. 2). IlTAL and FjTAL represent the two largest clusters with only uncharacterized coding sequences in the analysis (Table 4), and only the former cluster contains homologs linked to 4CL homologs.

Prediction of enzyme specificity from sequence or synteny. Aromatic amino acid ammonia-lyases and mutases share a range of residues that have been shown through structural studies, mutational analysis, and simulation to be important for substrate binding and catalysis (see Fig. S1 in the supplemental material) (36, 72, 73). Catalysis requires the formation of MIO and tyrosine residues Y60 and Y300 (RsTAL numbering) (26), and the MIO interacts with several other amino acid side chains and residues, including L153, G204, F350, and Q436 (22), which are all conserved in the selected enzymes.

Substrate binding takes place to accommodate the carboxylic acid group through R303 and N435 and the aliphatic part through Y60 and G67 to the ring structure through L90, L153, M405, N432, and Q436. The far end of the substrate binding pocket may be hydrophobic in the case of phenylalanine or hydrophilic in the case of tyrosine or histidine as a result of the presence of either aliphatic residues or charged residues (H89 and L90 in RsTAL). Mutational studies have confirmed that this last region is important for specificity and that this may be changed through mutation (22, 23). We included the RtXAL–RM120-1 mutant, where a mutation in this site resulted in increased specificity for tyrosine. The residues in this region are, however, not sufficient for predicting the substrate specificity. FjTAL, for example, has the highest sequence similarity to HALs and TAMs, while S_BagA, IlTAL, HaTAL1, and HaTAL2 do not conform to any of the previously defined sequences. Mutation of V409 has also been found to change the substrate specificity (60); however, this amino acid is not conserved within enzymes of the same specificity. A reaction mechanism has also been hypothesized to be determined by N432, which was an asparagine for TALs and TAMs and a glutamine for PALs and PAMs (28). However, there is no such consistency between substrate specificity and this residue for the newly identified enzymes, since S_BagA, IlTAL, HaTAL1, and HaTAL2 contain a glutamine in this position. The N435-Q436 dyad does, however, appear to allow a sequence-based distinction between HALs (QE or TE sequence) and all other enzymes (NQ).

The enzymes with dual TAL and PAL activity were generally of eukaryotic origin, although the bacterial R_XAL was capable of both reactions. We speculate that bacterial enzymes are more specific, as they take part in secondary metabolite formation, where the product is generally linked to a single downstream reaction.

FjTAL, whose specificity could not be inferred from phylogeny or primary sequence, may be involved in the formation of flexirubin pigments in *F. johnsoniae*, giving rise to the bacterium's yellow color, as it is found close to genes characteristic of flexirubin biosynthesis (74, 75). The gene encoding BlPAL, which shows homology to the TAL BagA, is present in a genomic region encoding polyketide synthases. HaTAL1 and HaTAL2 are very similar, while the third homolog encoded in the genome is more distinct and is

associated with histidine degradation. However, none of three TAL homologs present in the *Herpetosiphon aurantiacus* genome belongs to the proposed biosynthetic loci (76). Since sequence motifs as well as synteny were not sufficient to predict substrate specificity for all proposed enzymes, we performed an *in vivo* screening.

Screening for *p*-coumaric acid production in *Escherichia coli*. The coding sequences of all selected proteins were codon optimized and expressed in an *E. coli* B strain that was grown in minimal medium optionally supplemented with a 2 mM concentration of either tyrosine, phenylalanine, or histidine, and the resulting supernatants were analyzed for pHCA and CA formation (Fig. 3A). We were able to measure product formation for all enzymes except L_XAL and SrXAL. The enzymes RsTAL, RcTAL-var1, RcTAL-var2, R_TAL, IlTAL, S_BagA, SeSam8, LbTAL, HaTAL1, HaTAL2, and FjTAL all had TAL activities more than 10-fold higher than their PAL activities, except for R_XAL. The two variant enzymes from *R. capsulatus* shared a TAL-over-PAL preference, but one variant (RcTAL-var1) resulted in a 4-fold-higher specific production than the other despite only small sequence differences. RcTAL-var1 has a ten-amino-acid N-terminal extension, a single residue change, and a single residue gap near the C-terminal end compared to RcTAL-var2. The exogenous addition of the substrate tyrosine or phenylalanine to the growth medium caused an increased production of the products pHCA and CA, respectively (see Table S3 in the supplemental material). We also tested histidine as a potential substrate, but no urocanic acid was formed (data not shown), confirming that none of the selected enzymes had HAL activity when the genes were heterologously expressed. The highest production of pHCA was observed from the strains expressing SeSam8, FjTAL, and HaTAL1, with concentrations of 0.54, 0.44, and 0.13 mM pHCA OD_{600} unit^{-1} (1.6, 1.3, and 0.38 mmol pHCA [g CDW]$^{-1}$) while producing 18, 0.5, and 1.1 μM CA OD_{600} unit^{-1} (55, 1.5, and 3.2 μmol CA [g CDW]$^{-1}$), respectively. In order to determine the maximum rate of catalysis under the chosen reaction conditions, we followed the *in vivo* production of pHCA from *E. coli* after induction in late exponential growth phase with exogenous tyrosine added. The results (Fig. 4) show patterns similar to those obtained with the endpoint data (Fig. 3) and also show that SeSam8 and FjTAL are equally effective, while HaTAL1 produces pHCA at a rate around one third that of the other enzymes. SeSam8 and FjTal show pHCA productivities (43 $\pm$ 12 μM OD_{600} unit^{-1} h^{-1} and 36 $\pm$ 4.2 μM OD_{600} unit^{-1} h^{-1}) that were not significantly different, while HaTAL1 gave a significantly lower productivity (6.2 $\pm$ 0.53 μM OD_{600} unit^{-1} h^{-1}).

The yeast enzymes RmXAL, TcXAL, PcXAL, and RtXAL had almost equal TAL and PAL activities, given the substrate availability and product secretion *in vivo*. RtXAL had almost equal preference for the TAL and PAL reactions, in accordance with published results, and while one of the mutants, RtXAL-EP18Km-6, showed little difference in production from the wild type, the other mutant, RtXAL-RM120-1, had a clearly altered preference for the TAL reaction, as expected, but also an 86% diminished overall activity. Lastly, BlPAL, PpPAL, and DdPAL all exclusively had PAL activity. Based on whether there was a >10-fold preference for a reaction, we designated the enzymes as TAL, PAL, or XAL (less than 10-fold preference for either) (see Fig. S3 in the supplemental material).

Phylogenetically, HAL enzymes form a cluster separate from other enzymes (Fig. 2). Ritter and Schulz proposed that the eukary-
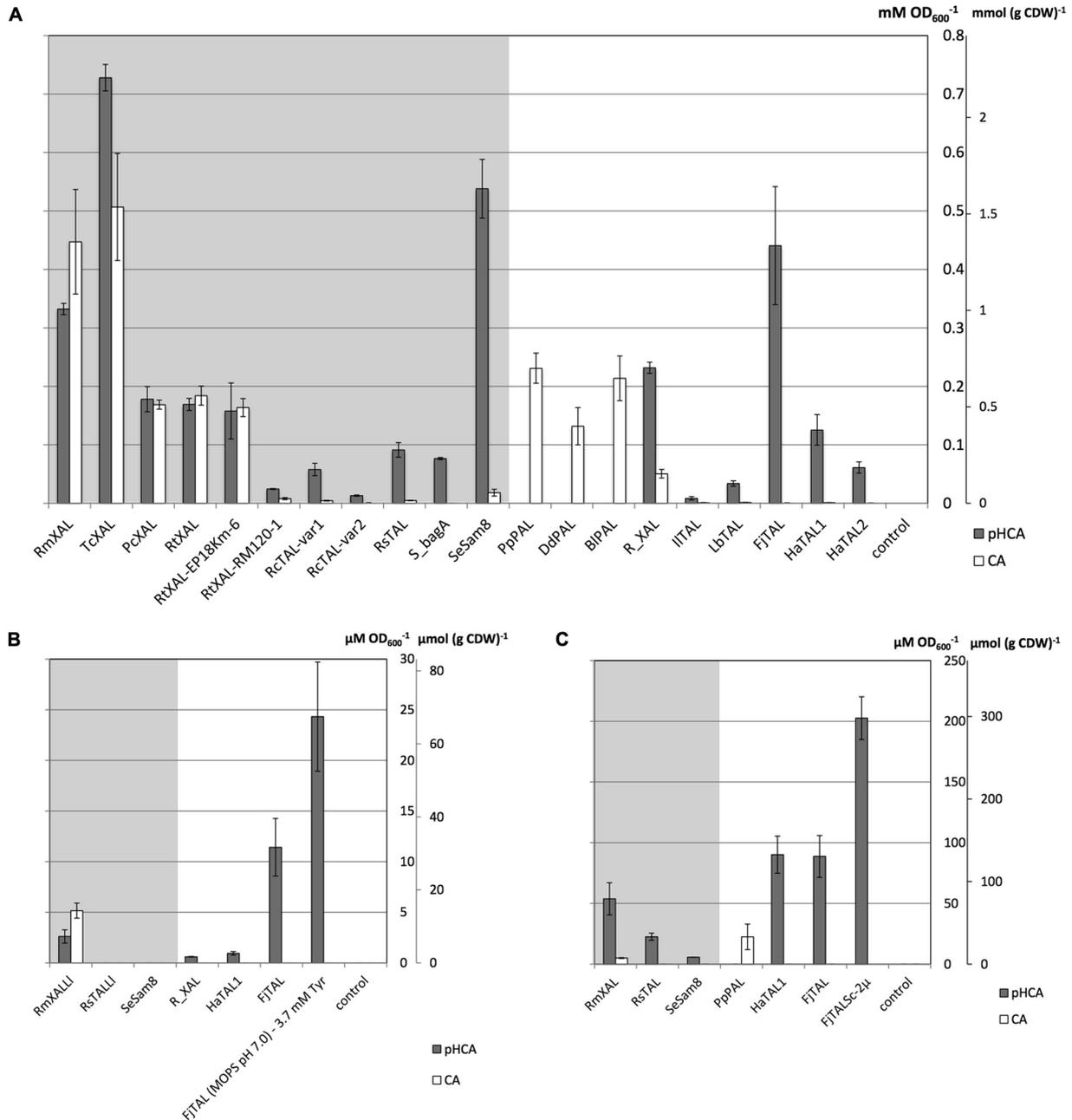
FIG 3 Production of *p*-coumaric acid (pHCA) and cinnamic acid (CA) in *E. coli*, *L. lactis*, and *S. cerevisiae* expressing aromatic amino acid ammonia-lyases. (A) Twenty-two open reading frames, codon optimized for *E. coli*, were expressed in *E. coli*. The pHCA and CA titers were measured from culture supernatants of cells grown in M9 minimal medium with glucose and supplemented with 2 mM tyrosine or phenylalanine, respectively. Some enzymes had both phenylalanine ammonia-lyase activity (PAL) and tyrosine ammonia-lyase activity (TAL), while others showed a high degree of substrate specificity. A gray background indicates enzymes previously studied in literature and also examined here. (B) Selected genes were expressed in *L. lactis* grown in medium containing both phenylalanine and tyrosine (1.7 mM). The pHCA production was increased when the cells were grown in medium with MOPS (morpholinepropanesulfonic acid) and adjusted to pH 7. (C) Genes were also expressed chromosomally in *S. cerevisiae* from the TEF1 promoter. Titers are from growth in synthetic fed-batch medium with the addition of either tyrosine or phenylalanine. The pHCA production was increased when the gene encoding FjTAL was codon optimized for *S. cerevisiae* and expressed from the PGK1 promoter on an episomal plasmid (FjTALSc-2μ). "Control" indicates the titers reached from a strain containing the native plasmid with no gene inserted or from *S. cerevisiae* without a gene integrated.

otic PALs evolved from a bacterial HAL early in time, while the bacterial PAL/TALs emerged independently later, also from bacterial HALs (38). The cyanobacterial PALs have been suggested to be related to an intermediate in this evolution (24). The previously described homologs from the cyanobacteria *Anabaena variabilis*

(AvPAL) and *Nostoc punctiforme* (NpPAL) have not had any measurable TAL activity (24), yet we identified the TALs, HaTAL1 and HaTAL2, that show greater sequence similarity to AvPAL and NpPAL than to any previously characterized TALs, suggesting that there has been convergent evolution of TAL and PAL activity.
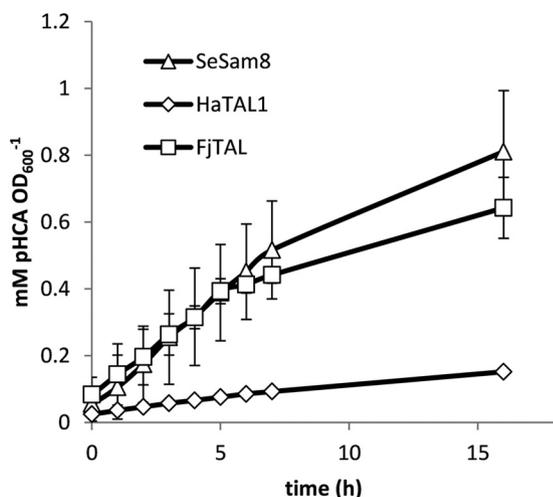
FIG 4 Production of pHCA in *E. coli* with tyrosine ammonia-lyases SeSam8, HaTAL1, and FjTAL. Genes encoding SeSam8, HaTAL1, or FjTAL were induced in cells after 3 h of growth in M9 minimal medium with glucose. After another 4 h, in the late exponential phase, tyrosine was added to 2 mM (time zero). The cell density reached stationary phase (OD_{600} of around 1.4) within 2 h thereafter.

The included plant enzyme, PpPAL from moss, clusters together with other plant enzymes that generally have a preference for the PAL reaction over the TAL reaction, and this enzyme shows a perfect specificity for phenylalanine. The PAL from *D. discoideum* (DdPAL) is shorter (529 amino acids) than the previously described PAL enzymes of eukaryotes (over 700 amino acids), as it lacks around 50 residues in the N-terminal end and around 180 residues in the C-terminal region compared to others (see Table S2 in the supplemental material). Its closest known homolog (49% identity) is the bacterial PAL enzyme StlA (19). The amoeba has been suggested to have acquired other prokaryotic genes by horizontal gene transfer (77), and this also is a likely origin of DdPAL.

Since substrate specificity is important for product purity, previous work focused on changing the specificity of yeast enzymes for the TAL reaction. RtXAL-RM120-1 did appear to have a higher TAL/PAL ratio than its parent (0.9 versus 3.0), but this ratio was still lower than what was observed for the novel bacterial enzymes, FjTAL and HaTAL1, where only trace amounts of CA could be detected.

Kinetic characterization of selected TAL enzymes. We further wanted to examine if the *in vivo* production observed in *E. coli* reflected the enzyme kinetic parameters, as the apparent *in vivo* activity also reflects substrate availability and product secretion. SeSam8, FjTAL, and HaTAL1, which showed the highest *in vivo* TAL activity while still being specific, were examined together with the previously characterized enzyme RsTAL. The four enzymes were purified or partially purified by identical means using N-terminal histidine tagging (19, 26) (see Fig. S2 in the supplemental material).

After the tyrosine concentration that resulted in maximal activity with a given enzyme concentration had been determined, the pH optima of RsTAL and SeSam8 and the novel enzymes HaTAL1 and FjTAL were determined (Fig. 5). The maximal enzymatic activities were found at pH 9.0 or above, where they were found to level off for all enzymes except HaTAL1, which showed a
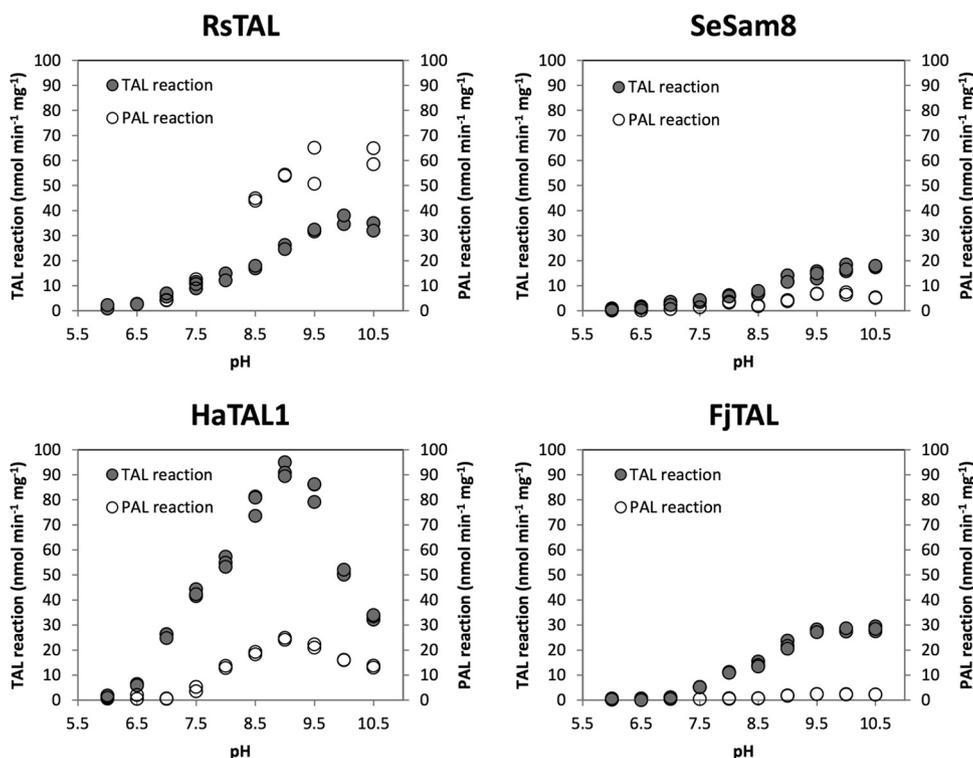

FIG 5 pH optima for RsTAL, SeSam8, HaTAL1, and FjTAL. The pH optima for the TAL and PAL reactions were measured from pH 6.0 to 10.5 in 0.5-pH-unit intervals and expressed as nanomoles of product produced per minute per milligram of protein.

TABLE 6 Kinetic analysis of four selected TAL homologs using tyrosine or phenylalanine as the substrate

Enzyme (organism)	Substrate	K_m (μM)	k_{cat} (s^{-1})	k_{cat}/K_m (mM^{-1} s^{-1})	TAL/PAL	Reference or source[a]
RsTAL (*Rhodobacter sphaeroides*)	Tyr	8.4	0.026	2.38	88	This work
	Phe	2100	0.075	0.0272		
SeSam8 (*Saccharothrix espanaensis*)	Tyr	4.7	0.015	3.05	1,200	This work
	Phe	6300	0.016	0.00249		
HaTAL1 (*Herpetosiphon auranticus*)	Tyr	24	0.076	2.74	500	This work
	Phe	33000	0.21	0.00552		
FjTAL (*Flavobacterium johnsoniae*)	Tyr	6.7	0.023	2.99	2,400	This work
	Phe	6600	0.0094	0.00123		
RsTAL[b] (*Rhodobacter sphaeroides*)	Tyr	74.2	4.32	1.15	51	22
	Phe	11400	13.1	58.2		
RsTAL[b] (*Rhodobacter sphaeroides*)	Tyr	31.4	3.4	108	268	23
	Phe	5204	2.1	0.404		
RsTAL[b] (*Rhodobacter sphaeroides*)	Tyr	60	0.02	0.333	19	60
	Phe	560	0.01	0.018		
RsTAL[b] (*Rhodobacter sphaeroides*)	Tyr	301	0.08	0.265	90	26
	Phe	6170	0.02	0.00297		
RsTAL[b] (*Rhodobacter sphaeroides*)	Tyr	100	0.9	10	44	28
	Phe	2700	0.6	0.226		
SeSam8 (*Saccharothrix espanaensis*)	Tyr	15.5	0.015	0.968	728	21
	Phe	2860	0.0038	0.00133		

[a] Data from literature were added for comparison for the previously characterized enzymes RsTAL and SeSam8.
[b] RsTAL from the literature (GI 46193106) differs in 8 positions from the RsTAL in this study.

decrease in activity at high pH. Similar pH optima were observed for the PAL and TAL reactions. The TAL activity was highest for HaTAL1 and lowest for SeSam8, reaching 95 and 18 nmol mg^{-1} min^{-1}, respectively. The PAL activity was highest for RsTAL and lowest for FjTAL, reaching 65 and 2 nmol mg^{-1} min^{-1}, respectively, in the presence of 6 mM phenylalanine.

The kinetic constants K_m and V_{max} were determined for the enzymes with either tyrosine or phenylalanine as a substrate at their optimal pH, as summarized in Table 6. SeSam8, HaTAL1, and FjTAL had very little activity for phenylalanine, with k_{cat}/K_m values of 2.49, 5.52, and 1.23 M^{-1} s^{-1}, respectively. HaTAL1 had high turnover numbers for both tyrosine (0.076 s^{-1}) and phenyl-alanine (0.21 s^{-1}) but very low affinity for phenylalanine (33 mM). FjTAL was the enzyme with the lowest activity for phenyl-alanine, resulting in a 2,400-fold-higher specificity constant, k_{cat}/K_m, between the two substrates. In comparison, SeSam8 was found to have a 1,200-fold difference in specificity between the substrates.

The kinetic constants are in line with previous analysis of SeSam8 (21), but the importance of standardized assays is evident when data for RsTAL in the literature, where dramatically different kinetic constants for the same enzyme have been presented, are compared (Table 6). These differences may have been due to different expression and assay conditions.

The high pH optimum of the reactions may be a reflection of the reaction mechanism and is generally identical for all enzymes and similar to what has been observed previously for RsTAL,

SeSam8, and other homologous enzymes (18, 20, 21, 23, 27, 78–81). Alkaline pH may also be used for biocatalysis, where tyrosine produced by fermentation at physiological pH can be converted to pHCA in high titers by subsequent reaction at alkaline pH in the presence of TAL-expressing *E. coli* cells or cell paste (82).

Production of *p*-coumaric acid in *Lactococcus lactis*. The performance of the novel enzymes were tested in a Gram-positive bacterium. Genes encoding HaTAL1, FjTAL, and four other en-zymes with TAL activity in *E. coli* were expressed individually in *L. lactis* from plasmids using a nisin-inducible promoter, and the production was measured in culture supernatants (Fig. 3B). Even though the genes encoding RsTAL and RmXAL had been specifi-cally codon optimized for *L. lactis*, RsTAL$_{Ll}$ and RmXAL$_{Ll}$, FjTAL showed by far the highest specific production of pHCA (15 μM OD$_{600}$ unit^{-1}, 43 μmol [g CDW]$^{-1}$), a 5-fold increase in specific production over RmXAL$_{Ll}$, the second-best enzyme. The values were lower than those achieved in *E. coli*, and the production of pHCA could be slightly increased when the concentration of ty-rosine in the medium was increased from 1.7 mM to 3.7 mM and the pH of the medium was increased from 6.5 to 7.0. RmXAL$_{Ll}$ was the only enzyme resulting in production of CA (see Table S3 in the supplemental material).

Production of *p*-coumaric acid in *Saccharomyces cerevisiae*. Yeasts, and in particular *S. cerevisiae*, are widely used as a cell factory for production of various chemicals (83). However, all known TAL enzymes of fungal origin also have at least a partial PAL activity. Well-described examples include enzymes used in

this study: RmXAL, TcXAL, PcXAL, and RtXAL. Twenty-one genes were cloned and were chromosomally integrated into *S. cerevisiae* and/or expressed from an episomal plasmid based on a 2μ origin of replication. The resulting strains were analyzed for production of CA and pHCA in minimal defined medium and in FIT fed-batch-simulation medium with or without addition of tyrosine or phenylalanine (see Table S3 in the supplemental material).

The novel enzymes HaTAL1 and FjTAL resulted in the highest production of pHCA, 90 and 89 μM pHCA OD_{600} $unit^{-1}$ (133 and 130 μmol pHCA $[g\ CDW]^{-1}$) (Fig. 3C; also, see Table S3 in the supplemental material) while remaining highly specific for the TAL reaction over the PAL reaction, as no CA could be detected. The specific production was almost 4-fold higher than what was obtained using the previously reported TAL, RsTAL (23 μM pHCA OD_{600} $unit^{-1}$; 33 μmol pHCA $[g\ CDW]^{-1}$).

As for *E. coli*, expression of genes encoding PpPAL, DdPAL, and BlPAL gave CA as the sole product, while PpPAL gave the highest specific production of CA (22 μM OD_{600} $unit^{-1}$; 33 μmol CA $[g\ CDW]^{-1}$). RmXAL led to production of both pHCA and CA, favoring pHCA, in contrast to the result for *E. coli* and *L. lactis*, where the CA production was equal or higher. RsTAL, S_BagA, SeSam8, R_XAL, IlTAL, LbTAL, FjTAL, and HaTAL1 all gave pHCA as the sole product, unlike in *E. coli*, where trace amounts of CA could be measured from all enzymes. The titers in defined minimal medium could be increased by the addition of phenylalanine or tyrosine, while the extent was less significant in the FIT medium. An analysis of the dynamics of pHCA production in FIT medium (see Fig. S4 in the supplemental material) by five strains expressing either of RsTAL, S_BagA, RmXAL, HaTAL1, or FjTAL revealed that additionally supplemented tyrosine was consumed fast by *S. cerevisiae*, without a significant simultaneous production of pHCA. Rather, the majority of the pHCA production was observed in the subsequent part of the growth experiment. Consumption of tyrosine without comparative production of the downstream pathway has previously been seen for resveratrol production in yeast (84). In *S. cerevisiae*, the previously best-performing TAL enzymes have been reported to be those from *Rhodosporidium* (RtXAL) (3, 85) and *Rhodobacter* (RcTAL and RsTAL) (7, 9). In comparison, the novel FjTAL and HaTAL1 enzymes gave a specific pHCA production that was three- to fivefold higher while not resulting in any measurable production of CA as a side product (see Table S3 in the supplemental material). The production was further increased by codon optimizing the genes encoding HaTAL1 and FjTAL for *S. cerevisiae* and expressing these from an episomal plasmid (see Table S3 in the supplemental material). The most significant improvements were observed for FjTAL (Fig. 3C), reaching 200 μM OD_{600} $unit^{-1}$ (300 μmol $[g\ CDW]^{-1}$) in FIT medium supplemented with tyrosine.

Conclusion. In conclusion, 22 TAL and PAL genes were expressed and screened for product formation in *E. coli*. Selected enzymes were purified and characterized kinetically, and their efficacy was further demonstrated in the industrially important Gram-positive bacterium *L. lactis* as well as in the yeast *S. cerevisiae*. To our knowledge, this constitutes the largest comparative study of TAL homologs for biotechnological purposes reported so far, and it sheds light on the broader phylogenetic distribution of TAL and PAL activities, as the novel enzymes presented here cover a portion of the sequence space not previously covered by characterized enzymes. The study resulted in the identification of enzymes with improved kinetic characteristics over the currently

employed enzymes. The novel TALs outperformed the previously characterized TALs when employed *in vivo* in a Gram-negative bacterium, a Gram-positive bacterium, and a yeast, while being very specific, as confirmed by *in vitro* kinetic experiments. We envision a role of the presented enzymes in biochemical production of phenolic compounds, and we are currently employing them in a series of cell factory designs.

REFERENCES

1. Watts KT, Lee PC, Schmidt-Dannert C. 2004. Exploring recombinant flavonoid biosynthesis in metabolically engineered *Escherichia coli*. Chembiochem **5**:500–507. http://dx.doi.org/10.1002/cbic.200300783.
2. Yan Y, Kohli A, Koffas MA. 2005. Biosynthesis of natural flavanones in *Saccharomyces cerevisiae*. Appl Environ Microbiol **71**:5610–5613. http://dx.doi.org/10.1128/AEM.71.9.5610-5613.2005.
3. Vannelli T, Wei Qi W, Sweigard J, Gatenby AA, Sariaslani FS. 2007. Production of *p*-hydroxycinnamic acid from glucose in *Saccharomyces cerevisiae* and *Escherichia coli* by expression of heterologous genes from plants and fungi. Metab Eng **9**:142–151. http://dx.doi.org/10.1016/j.ymben.2006.11.001.
4. Xue Y, Zhang Y, Cheng D, Daddy S, He Q. 2014. Genetically engineering *Synechocystis* sp. Pasteur Culture Collection 6803 for the sustainable production of the plant secondary metabolite *p*-coumaric acid. Proc Natl Acad Sci U S A **111**:9449–9454. http://dx.doi.org/10.1073/pnas.1323725111.
5. Nijkamp K, Westerhof RG, Ballerstedt H, de Bont JA, Wery J. 2007. Optimization of the solvent-tolerant *Pseudomonas putida* S12 as host for the production of *p*-coumarate from glucose. Appl Microbiol Biotechnol **74**:617–624. http://dx.doi.org/10.1007/s00253-006-0703-0.
6. Wu J, Liu P, Fan Y, Bao H, Du G, Zhou J, Chen J. 2013. Multivariate modular metabolic engineering of *Escherichia coli* to produce resveratrol from L-tyrosine. J Biotechnol **167**:404–411. http://dx.doi.org/10.1016/j.jbiotec.2013.07.030.
7. Wang Y, Halls C, Zhang J, Matsuno M, Zhang Y, Yu O. 2011. Stepwise increase of resveratrol biosynthesis in yeast *Saccharomyces cerevisiae* by metabolic engineering. Metab Eng **13**:455–463. http://dx.doi.org/10.1016/j.ymben.2011.04.005.
8. Santos CN, Koffas M, Stephanopoulos G. 2011. Optimization of a heterologous pathway for the production of flavonoids from glucose. Metab Eng **13**:392–400. http://dx.doi.org/10.1016/j.ymben.2011.02.002.
9. Koopman F, Beekwilder J, Crimi B, van Houwelingen A, Hall RD, Bosch D, van Maris AJ, Pronk JT, Daran JM. 2012. *De novo* production of the flavonoid naringenin in engineered *Saccharomyces cerevisiae*. Microb Cell Fact **11**:155. http://dx.doi.org/10.1186/1475-2859-11-155.
10. Eudes A, Juminaga D, Baidoo EE, Collins FW, Keasling JD, Loqué D. 2013. Production of hydroxycinnamoyl anthranilates from glucose in *Escherichia coli*. Microb Cell Fact **12**:62. http://dx.doi.org/10.1186/1475-2859-12-62.
11. Qi WW, Vannelli T, Breinig S, Ben-Bassat A, Gatenby AA, Haynie SL, Sariaslani FS. 2007. Functional expression of prokaryotic and eukaryotic genes in *Escherichia coli* for conversion of glucose to *p*-hydroxystyrene. Metab Eng **9**:268–276. http://dx.doi.org/10.1016/j.ymben.2007.01.002.
12. Verhoef S, Wierckx N, Westerhof RG, de Winde JH, Ruijssenaars HJ. 2009. Bioproduction of *p*-hydroxystyrene from glucose by the solvent-tolerant bacterium *Pseudomonas putida* S12 in a two-phase water-decanol fermentation. Appl Environ Microbiol **75**:931–936. http://dx.doi.org/10.1128/AEM.02186-08.
13. Lin Y, Yan Y. 2012. Biosynthesis of caffeic acid in *Escherichia coli* using its endogenous hydroxylase complex. Microb Cell Fact **11**:42. http://dx.doi.org/10.1186/1475-2859-11-42.
14. Appert C, Logemann E, Hahlbrock K, Schmid J, Amrhein N. 1994. Structural and catalytic properties of the four phenylalanine ammonia-lyase isoen-

zymes from parsley (*Petroselinum crispum* Nym.). Eur J Biochem **225**:491–499. http://dx.doi.org/10.1111/j.1432-1033.1994.00491.x.

15. **Schuster B, Rétey J.** 1995. The mechanism of action of phenylalanine ammonia-lyase: the role of prosthetic dehydroalanine. Proc Natl Acad Sci U S A **92**:8433–8437. http://dx.doi.org/10.1073/pnas.92.18.8433.

16. **Rösler J, Krekel F, Amrhein N, Schmid J.** 1997. Maize phenylalanine ammonia-lyase has tyrosine ammonia-lyase activity. Plant Physiol **113**:175–179. http://dx.doi.org/10.1104/pp.113.1.175.

17. **Gatenby AA, Sariaslani FS, Tang X, Qi WW, Vannelli T.** April 2002. Bioproduction of para-hydroxycinnamic acid. US patent US6368837 B1.

18. **Kyndt JA, Meyer TE, Cusanovich MA, Van Beeumen JJ.** 2002. Characterization of a bacterial tyrosine ammonia lyase, a biosynthetic enzyme for the photoactive yellow protein. FEBS Lett **512**:240–244. http://dx.doi.org/10.1016/S0014-5793(02)02272-X.

19. **Williams JS, Thomas M, Clarke DJ.** 2005. The gene *stlA* encodes a phenylalanine ammonia-lyase that is involved in the production of a stilbene antibiotic in *Photorhabdus luminescens* TT01. Microbiology **151**:2543–2550. http://dx.doi.org/10.1099/mic.0.28136-0.

20. **Xiang LK, Moore BS.** 2005. Biochemical characterization of a prokaryotic phenylalanine ammonia lyase. J Bacteriol **187**:4286–4289. http://dx.doi.org/10.1128/JB.187.12.4286-4289.2005.

21. **Berner M, Krug D, Bihlmaier C, Vente A, Müller R, Bechthold A.** 2006. Genes and enzymes involved in caffeic acid biosynthesis in the actinomycete *Saccharothrix espanaensis*. J Bacteriol **188**:2666–2673. http://dx.doi.org/10.1128/JB.188.7.2666-2673.2006.

22. **Louie GV, Bowman ME, Moffitt MC, Baiga TJ, Moore BS, Noel JP.** 2006. Structural determinants and modulation of substrate specificity in phenylalanine-tyrosine ammonia-lyases. Chem Biol **13**:1327–1338. http://dx.doi.org/10.1016/j.chembiol.2006.11.011.

23. **Watts KT, Mijts BN, Lee PC, Manning AJ, Schmidt-Dannert C.** 2006. Discovery of a substrate selectivity switch in tyrosine ammonia-lyase, a member of the aromatic amino acid lyase family. Chem Biol **13**:1317–1326. http://dx.doi.org/10.1016/j.chembiol.2006.10.008.

24. **Moffitt MC, Louie GV, Bowman ME, Pence J, Noel JP, Moore BS.** 2007. Discovery of two cyanobacterial phenylalanine ammonia lyases: kinetic and structural characterization. Biochemistry **46**:1004–1012. http://dx.doi.org/10.1021/bi061774g.

25. **Vannelli T, Xue Z, Breinig S, Qi WW, Sariaslani FS.** 2007. Functional expression in *Escherichia coli* of the tyrosine-inducible tyrosine ammonia-lyase enzyme from yeast *Trichosporon cutaneum* for production of *p*-hydroxycinnamic acid. Enzyme Microb Technol **41**:413–422. http://dx.doi.org/10.1016/j.enzmictec.2007.03.013.

26. **Schroeder AC, Kumaran S, Hicks LM, Cahoon RE, Halls C, Yu O, Jez JM.** 2008. Contributions of conserved serine and tyrosine residues to catalysis, ligand binding, and cofactor processing in the active site of tyrosine ammonia lyase. Phytochemistry **69**:1496–1506. http://dx.doi.org/10.1016/j.phytochem.2008.02.007.

27. **Wang L, Gamez A, Archer H, Abola EE, Sarkissian CN, Fitzpatrick P, Wendt D, Zhang Y, Vellard M, Bliesath J, Bell SM, Lemontt JF, Scriver CR, Stevens RC.** 2008. Structural and biochemical characterization of the therapeutic *Anabaena variabilis* phenylalanine ammonia lyase. J Mol Biol **380**:623–635. http://dx.doi.org/10.1016/j.jmb.2008.05.025.

28. **Bartsch S, Bornscheuer UT.** 2009. A single residue influences the reaction mechanism of ammonia lyases and mutases. Angew Chem Int Ed Engl **48**:3362–3365. http://dx.doi.org/10.1002/anie.200900337.

29. **Krug D, Müller R.** 2009. Discovery of additional members of the tyrosine aminomutase enzyme family and the mutational analysis of CmdF. Chembiochem **10**:741–750. http://dx.doi.org/10.1002/cbic.200800748.

30. **Bartsch S, Bornscheuer UT.** 2010. Mutational analysis of phenylalanine ammonia lyase to improve reactions rates for various substrates. Protein Eng Des Sel **23**:929–933. http://dx.doi.org/10.1093/protein/gzq089.

31. **Hsieh LS, Yeh CS, Pan HC, Cheng CY, Yang CC, Lee PD.** 2010. Cloning and expression of a phenylalanine ammonia-lyase gene (BoPAL2) from *Bambusa oldhamii* in *Escherichia coli* and *Pichia pastoris*. Protein Expr Purif **71**:224–230. http://dx.doi.org/10.1016/j.pep.2010.01.009.

32. **Zhu L, Cui W, Fang Y, Liu Y, Gao X, Zhou Z.** 2013. Cloning, expression and characterization of phenylalanine ammonia-lyase from *Rhodotorula glutinis*. Biotechnol Lett **35**:751–756. http://dx.doi.org/10.1007/s10529-013-1140-7.

33. **Christenson SD, Liu W, Toney MD, Shen B.** 2003. A novel 4-methylideneimidazole-5-one-containing tyrosine aminomutase in enediyne antitumor antibiotic C-1027 biosynthesis. J Am Chem Soc **125**:6062–6063. http://dx.doi.org/10.1021/ja034609m.

34. **Jin M, Fischbach MA, Clardy J.** 2006. A biosynthetic gene cluster for the acetyl-CoA carboxylase inhibitor andrimid. J Am Chem Soc **128**:10660–10661. http://dx.doi.org/10.1021/ja063194c.

35. **Rachid S, Krug D, Weissman KJ, Müller R.** 2007. Biosynthesis of (*R*)-β-tyrosine and its incorporation into the highly cytotoxic chondramides produced by *Chondromyces crocatus*. J Biol Chem **282**:21810–21817. http://dx.doi.org/10.1074/jbc.M703439200.

36. **Schwede TF, Rétey J, Schulz GE.** 1999. Crystal structure of histidine ammonia-lyase revealing a novel polypeptide modification as the catalytic electrophile. Biochemistry **38**:5355–5361. http://dx.doi.org/10.1021/bi982929q.

37. **Calabrese JC, Jordan DB, Boodhoo A, Sariaslani S, Vannelli T.** 2004. Crystal structure of phenylalanine ammonia lyase: multiple helix dipoles implicated in catalysis. Biochemistry **43**:11403–11416. http://dx.doi.org/10.1021/bi049053+.

38. **Ritter H, Schulz GE.** 2004. Structural basis for the entrance into the phenylpropanoid metabolism catalyzed by phenylalanine ammonia-lyase. Plant Cell **16**:3426–3436. http://dx.doi.org/10.1105/tpc.104.025288.

39. **Huang L, Xue Z.** June 2006. DNA and amino acid sequence of a tyrosine ammonia lyase enzyme from the bacterium *Rhodobacter sphaeroides*. US patent US7067302 B2.

40. **Zhu Y, Liao S, Ye J, Zhang H.** 2012. Cloning and characterization of a novel tyrosine ammonia lyase-encoding gene involved in bagremycins biosynthesis in *Streptomyces* sp. Biotechnol Lett **34**:269–274. http://dx.doi.org/10.1007/s10529-011-0755-9.

41. **Vaslet C, Strausberg R, Sykes A, Levy A, Filpula D.** 1988. cDNA and genomic cloning of yeast phenylalanine ammonia-lyase genes reveal genomic intron deletions. Nucleic Acids Res **16**:11382–11382. http://dx.doi.org/10.1093/nar/16.23.11382.

42. **Filpula D, Vaslet CA, Levy A, Sykes A, Strausberg RL.** 1988. Nucleotide sequence of gene for phenylalanine ammonia-lyase from *Rhodotorula rubra*. Nucleic Acids Res **16**:11381. http://dx.doi.org/10.1093/nar/16.23.11381.

43. **Hwang EI, Kaneko M, Ohnishi Y, Horinouchi S.** 2003. Production of plant-specific flavanones by *Escherichia coli* containing an artificial gene cluster. Appl Environ Microbiol **69**:2699–2706. http://dx.doi.org/10.1128/AEM.69.5.2699-2706.2003.

44. **Huang Y, Niu B, Gao Y, Fu L, Li W.** 2010. CD-HIT suite: a web server for clustering and comparing biological sequences. Bioinformatics **26**:680–682. http://dx.doi.org/10.1093/bioinformatics/btq003.

45. **Grin I, Linke D.** 2011. GCView: the genomic context viewer for protein homology searches. Nucleic Acids Res **39**:W353–W356. http://dx.doi.org/10.1093/nar/gkr364.

46. **Tamura K, Stecher G, Peterson D, Filipski A, Kumar S.** 2013. MEGA6: Molecular Evolutionary Genetics Analysis version 6.0. Mol Biol Evol **30**:2725–2729. http://dx.doi.org/10.1093/molbev/mst197.

47. **Jones DT, Taylor WR, Thornton JM.** 1992. The rapid generation of mutation data matrices from protein sequences. Comput Appl Biosci **8**:275–282. http://dx.doi.org/10.1093/bioinformatics/8.3.275.

48. **Sievers F, Wilm A, Dineen D, Gibson TJ, Karplus K, Li W, Lopez R, McWilliam H, Remmert M, Söding J, Thompson JD, Higgins DG.** 2011. Fast, scalable generation of high-quality protein multiple sequence alignments using Clustal Omega. Mol Syst Biol **7**:539. http://dx.doi.org/10.1038/msb.2011.75.

49. **Jensen NB, Strucko T, Kildegaard KR, David F, Maury J, Mortensen UH, Förster J, Nielsen J, Borodina I.** 2014. EasyClone: method for iterative chromosomal integration of multiple genes in *Saccharomyces cerevisiae*. FEMS Yeast Res **14**:238–248. http://dx.doi.org/10.1111/1567-1364.12118.

50. **Verduyn C, Postma E, Scheffers WA, Van Dijken JP.** 1992. Effect of benzoic acid on metabolic fluxes in yeasts: a continuous-culture study on the regulation of respiration and alcoholic fermentation. Yeast **8**:501–517. http://dx.doi.org/10.1002/yea.320080703.

51. **Poolman B, Konings WN.** 1988. Relation of growth of *Streptococcus lactis* and *Streptococcus cremoris* to amino acid transport. J Bacteriol **170**:700–707.

52. **Sambrook J, Fritsch EF, Maniatis T.** 1989. Molecular cloning: a laboratory manual. Cold Spring Harbor Laboratory Press, Cold Spring Harbor, NY.

53. **Birnboim HC.** 1983. A rapid alkaline extraction method for the isolation of plasmid DNA. Methods Enzymol **100**:243–255. http://dx.doi.org/10.1016/0076-6879(83)00059-2.

54. **Geu-Flores F, Nour-Eldin HH, Nielsen MT, Halkier BA.** 2007. USER fusion: a rapid and efficient method for simultaneous fusion and cloning

of multiple PCR products. Nucleic Acids Res **35**:e55. http://dx.doi.org/10.1093/nar/gkm106.

55. **Gietz RD, Schiestl RH.** 2007. High-efficiency yeast transformation using the LiAc/SS carrier DNA/PEG method. Nat Protoc **2**:31–34. http://dx.doi.org/10.1038/nprot.2007.13.

56. **Kuipers OP, de Ruyter PGGA, Kleerebezem M, de Vos WM.** 1998. Quorum sensing-controlled gene expression in lactic acid bacteria. J Biotechnol **64**:15–21. http://dx.doi.org/10.1016/S0168-1656(98)00100-X.

57. **Holo H, Nes IF.** 1995. Transformation of *Lactococcus* by electroporation. Methods Mol Biol **47**:195–199. http://dx.doi.org/10.1385/0-89603-310-4:195.

58. **Sauer U, Lasko DR, Fiaux J, Hochuli M, Glaser R, Szyperski T, Wuthrich K, Bailey JE.** 1999. Metabolic flux ratio analysis of genetic and environmental modulations of *Escherichia coli* central carbon metabolism. J Bacteriol **181**:6679–6688.

59. **Gaspar P, Neves AR, Ramos A, Gasson MJ, Shearman CA, Santos H.** 2004. Engineering *Lactococcus lactis* for production of mannitol: high yields from food-grade strains deficient in lactate dehydrogenase and the mannitol transport system. Appl Environ Microbiol **70**:1466–1474. http://dx.doi.org/10.1128/AEM.70.3.1466-1474.2004.

60. **Xue Z, McCluskey M, Cantera K, Sariaslani FS, Huang L.** 2007. Identification, characterization and functional expression of a tyrosine ammonia-lyase and its mutants from the photosynthetic bacterium *Rhodobacter sphaeroides*. J Ind Microbiol Biotechnol **34**:599–604. http://dx.doi.org/10.1007/s10295-007-0229-1.

61. **Hodgins DS.** 1971. Yeast phenylalanine ammonia-lyase. Purification, properties, and the identification of catalytically essential dehydroalanine. J Biol Chem **246**:2977–2985.

62. **Anson JG, Gilbert HJ, Oram JD, Minton NP.** 1987. Complete nucleotide sequence of the *Rhodosporidium toruloides* gene coding for phenylalanine ammonia-lyase. Gene **58**:189–199. http://dx.doi.org/10.1016/0378-1119(87)90375-1.

63. **Strobel T, Al-Dilaimi A, Blom J, Gessner A, Kalinowski J, Luzhetska M, Pühler A, Szczepanowski R, Bechthold A, Rückert C.** 2012. Complete genome sequence of *Saccharothrix espanaensis* DSM 44229^T and comparison to the other completely sequenced *Pseudonocardiaceae*. BMC Genomics **13**:465. http://dx.doi.org/10.1186/1471-2164-13-465.

64. **Schomburg I, Chang A, Placzek S, Söhngen C, Rother M, Lang M, Munaretto C, Ulas S, Stelzer M, Grote A, Scheer M, Schomburg D.** 2013. BRENDA in 2013: integrated reactions, kinetic data, enzyme function data, improved disease classification: new options and contents in BRENDA. Nucleic Acids Res **41**:D764–D772. http://dx.doi.org/10.1093/nar/gks1049.

65. **Kyndt JA, Vanrobaeys F, Fitch JC, Devreese BV, Meyer TE, Cusanovich MA, Van Beeumen JJ.** 2003. Heterologous production of *Halorhodospira halophila* holo-photoactive yellow protein through tandem expression of the postulated biosynthetic genes. Biochemistry **42**:965–970. http://dx.doi.org/10.1021/bi027037b.

66. **Memmi S, Kyndt J, Meyer T, Devreese B, Cusanovich M, Van Beeumen J.** 2008. Photoactive yellow protein from the halophilic bacterium *Salinibacter ruber*. Biochemistry **47**:2014–2024. http://dx.doi.org/10.1021/bi701486n.

67. **Röther D, Poppe L, Viergutz S, Langer B, Rétey J.** 2001. Characterization of the active site of histidine ammonia-lyase from *Pseudomonas putida*. Eur J Biochem **268**:6011–6019. http://dx.doi.org/10.1046/j.0014-2956.2001.02298.x.

68. **Röther D, Poppe L, Morlock G, Viergutz S, Rétey J.** 2002. An active site homology model of phenylalanine ammonia-lyase from *Petroselinum crispum*. Eur J Biochem **269**:3065–3075. http://dx.doi.org/10.1046/j.1432-1033.2002.02984.x.

69. **Kawai Y, Noda S, Ogino C, Takeshima Y, Okai N, Tanaka T, Kondo A.** 2013. *p*-Hydroxycinnamic acid production directly from cellulose using endoglucanase- and tyrosine ammonia lyase-expressing *Streptomyces lividans*. Microb Cell Fact **12**:45. http://dx.doi.org/10.1186/1475-2859-12-45.

70. **Xue Z, McCluskey M, Cantera K, Ben-Bassat A, Sariaslani RS, Huang L.** 2007. Improved production of *p*-hydroxycinnamic acid from tyrosine using a novel thermostable phenylalanine/tyrosine ammonia lyase enzyme. Enzyme Microb Technol **42**:58–64. http://dx.doi.org/10.1016/j.enzmictec.2007.07.025.

71. **Tang X.** February 2003. Polynucleotide encoding a mutant *Rhodotorula glutinis* tyrosine ammonia lyase polypeptide. US patent US6521748 B2.

72. **Langer M, Reck G, Reed J, Rétey J.** 1994. Identification of serine-143 as the most likely precursor of dehydroalanine in the active site of histidine ammonia-lyase. A study of the overexpressed enzyme by site-directed mutagenesis. Biochemistry **33**:6462–6467. http://dx.doi.org/10.1021/bi00187a011.

73. **Pilbák S, Farkas O, Poppe L.** 2012. Mechanism of the tyrosine ammonia lyase reaction-tandem nucleophilic and electrophilic enhancement by a proton transfer. Chemistry **18**:7793–7802. http://dx.doi.org/10.1002/chem.201103662.

74. **Reichenbach H, Kohl W, Böttger-Vetter A, Achenbach H.** 1980. Flexirubin-type pigments in *Flavobacterium*. Arch Microbiol **126**:291–293. http://dx.doi.org/10.1007/BF00409934.

75. **McBride MJ, Xie G, Martens EC, Lapidus A, Henrissat B, Rhodes RG, Goltsman E, Wang W, Xu J, Hunnicutt DW, Staroscik AM, Hoover TR, Cheng YQ, Stein JL.** 2009. Novel features of the polysaccharide-digesting gliding bacterium *Flavobacterium johnsoniae* as revealed by genome sequence analysis. Appl Environ Microbiol **75**:6864–6875. http://dx.doi.org/10.1128/AEM.01495-09.

76. **Kiss H, Nett M, Domin N, Martin K, Maresca JA, Copeland A, Lapidus A, Lucas S, Berry KW, Glavina Del Rio T, Dalin E, Tice H, Pitluck S, Richardson P, Bruce D, Goodwin L, Han C, Detter JC, Schmutz J, Brettin T, Land M, Hauser L, Kyrpides NC, Ivanova N, Göker M, Woyke T, Klenk HP, Bryant DA.** 2011. Complete genome sequence of the filamentous gliding predatory bacterium *Herpetosiphon aurantiacus* type strain (114-95^T). Stand Genomic Sci **5**:356–370. http://dx.doi.org/10.4056/sigs.2194987.

77. **Eichinger L, Pachebat JA, Glöckner G, Rajandream MA, Sucgang R, Berriman M, Song J, Olsen R, Szafranski K, Xu Q, Tunggal B, Kummerfeld S, Madera M, Konfortov BA, Rivero F, Bankier AT, Lehmann R, Hamlin N, Davies R, Gaudet P, Fey P, Pilcher K, Chen G, Saunders D, Sodergren E, Davis P, Kerhornou A, Nie X, Hall N, Anjard C, Hemphill L, Bason N, Farbrother P, Desany B, Just E, Morio T, Rost R, Churcher C, Cooper J, Haydock S, van Driessche N, Cronin A, Goodhead I, Muzny D, Mourier T, Pain A, Lu M, Harper D, Lindsay R, Hauser H, et al.** 2005. The genome of the social amoeba *Dictyostelium discoideum*. Nature **435**:43–57. http://dx.doi.org/10.1038/nature03481.

78. **Kovács K, Bánóczi G, Varga A, Szabó I, Holczinger A, Hornyánszky G, Zagyva I, Paizs C, Vértessy BG, Poppe L.** 2014. Expression and properties of the highly alkalophilic phenylalanine ammonia-lyase of thermophilic *Rubrobacter xylanophilus*. PLoS One **9**:e85943. http://dx.doi.org/10.1371/journal.pone.0085943.

79. **Christenson SD, Wu W, Spies MA, Shen B, Toney MD.** 2003. Kinetic analysis of the 4-methylideneimidazole-5-one-containing tyrosine aminomutase in enediyne antitumor antibiotic C-1027 biosynthesis. Biochemistry **42**:12708–12718. http://dx.doi.org/10.1021/bi035223r.

80. **Hu GS, Jia JM, Hur YJ, Chung YS, Lee JH, Yun DJ, Chung WS, Yi GH, Kim TH, Kim DH.** 2011. Molecular characterization of phenylalanine ammonia lyase gene from *Cistanche deserticola*. Mol Biol Rep **38**:3741–3750. http://dx.doi.org/10.1007/s11033-010-0489-0.

81. **Gao ZM, Wang XC, Peng ZH, Zheng B, Liu Q.** 2012. Characterization and primary functional analysis of phenylalanine ammonia-lyase gene from *Phyllostachys edulis*. Plant Cell Rep **31**:1345–1356. http://dx.doi.org/10.1007/s00299-012-1253-9.

82. **Ben-Bassat A, Sariaslani FS, Huang L, Patnaik R, Lowe DJ.** August 2011. Methods for the preparation of para-hydroxycinnamic acid and cinnamic acid at alkaline pH. US patent US8003356 B2.

83. **Borodina I, Nielsen J.** 2014. Advances in metabolic engineering of yeast *Saccharomyces cerevisiae* for production of chemicals. Biotechnol J **9**:609–620. http://dx.doi.org/10.1002/biot.201300445.

84. **Shin SY, Jung SM, Kim MD, Han NS, Seo JH.** 2012. Production of resveratrol from tyrosine in metabolically engineered *Saccharomyces cerevisiae*. Enzyme Microb Technol **51**:211–216. http://dx.doi.org/10.1016/j.enzmictec.2012.06.005.

85. **Jiang H, Wood KV, Morgan JA.** 2005. Metabolic engineering of the phenylpropanoid pathway in *Saccharomyces cerevisiae*. Appl Environ Microbiol **71**:2962–2969. http://dx.doi.org/10.1128/AEM.71.6.2962-2969.2005.

86. **Gaspar P, Vieira A, Kuipers OP, Förster J, Neves AR.** 2013. Engineering *Lactococcus lactis* for the production of plant polyphenols. *In* Abstr Bio-MicroWorld 2013: V Int Conf Environ Ind Appl Microbiol, Madrid, Spain, 2 to 4 October 2013.